Journal of Sustainable Construction Materials and Technologies

Volume 7 | Issue 4 Article 5

2022

# A Review on Selected Durability Parameters on Performance of Geopolymers Containing Industrial By-products, Agro- Wastes and Natural Pozzolan

Festus Ngui
*Pwani University*

Najya Muhammed
*Pwani University*

Fredrick Mulei Mutunga
*Pwani University*

Joseph Marangu
*Meru University of Science & Technology*

Ismael Kithinji Kınotı
*Meru University of Science & Technology*

Journal of Sustainable Construction Materials and Technologies
Web page info: https://jscmt.yildiz.edu.tr
DOI: 10.47481/jscmt.1190244

JSCMT
Journal of Sustainable Construction Materials and Technologies

Review Article

# A review on selected durability parameters on performance of geopolymers containing industrial by-products, agro- wastes and natural pozzolan

**Festus Musyimi NGUI[*1], Najya MUHAMMED[1], Fredrick Mulei MUTUNGA[1], Joseph Mwiti MARANGU[2], Ismael Kithinji KINOTI[2]**

[1]*Department of Chemistry, Pwani University, Kilifi, Kenya*
[2]*Department of Physical Sciences, Meru University of Science & Technology, Meru, Kenya*

## ARTICLE INFO

*Article history*
Received: 18 October 2022
Revised: 19 November 2022
Accepted: 20 November 2022

**Key words:**
Agro-industrial waste, calcined clay, coconut ash, durability, geopolymer

## ABSTRACT

The applications of geopolymers as cementitious systems are becoming an alternative source of cement daily. The use of potentially suitable aluminosilicate inorganic waste materials incorporated with agro-industrial waste in the production of suitable geopolymer binders has been reported. Calcined clay and some agro-waste ash, such as coconut shells, are examples of aluminosilicate materials that exhibit strong pozzolanic activity because of their high silica-alumina composition. The pozzolanic reaction is primarily caused by the amorphous silica present in properly burned agricultural waste and clay. Based on a variety of available literature on concrete and mortar including geopolymers synthesized from the by-product and agro-industrial waste and natural pozzolan, a critical review of raw materials and the mechanism of synthesis of the geopolymer has been outlined in this work. Also, a brief review of the durability characteristics of this geopolymer concrete and mortar has been done. These include resistance to chloride, corrosion, sulphate and acid attack, depth of carbonation, thermal performance, Creep and drying shrinkage.

**Cite this article as:** Ngui, FM., Muhammed, N., Mutunga, FM., Marangu, JM., & Kinoti, IK. (2022). A review on selected durability parameters on performance of geopolymers containing industrial by-products, agro- wastes and natural pozzolan. *J Sustain Const Mater Technol*, 7(4), 375–400.

## 1. INTRODUCTION

The worldwide search for a sustainable and environmentally friendly alternative to today's dominant-natural resource-depleting convectional cement supply is the result of the rising binder innovations. Numerous agro-industrial byproducts and wastes as well as natural pozzolans have the potential to help resolve some of the world's binder and environmental issues due to their well-known silica and/or alumina content. Numerous agricultural wastes have indeed been reported to contain pozzolanic ash, including coconut shell/fiber, olive stones, sugar cane bagasse, cotton stalks, and grape seeds [1–4]. Other reported potential agro-waste are from pine sawdust, almond, nut, hazelnut, and sunflow-

***Corresponding author.**
*E-mail address: festongu@gmail.com

er shells, corn, oat, and rice hulls [5], apricot, peach, and cherry stones, sunflower stalk [5–9]. Amorphous silica and the reactive element in the ash can be utilized as pozzolan in cement manufacturing to provide inexpensive building blocks and as cement, in addition to hardening hazardous wastes [10–12]. Recent studies have shown that some of the ashes can be used to create geopolymer and alkali-activated materials (AAMs) [13].

Geopolymer is an aluminosilicate binder that is made by the use of alkaline as an activator on solid precursor materials that contain silica and alumina at or just above room temperature. The alkaline solution is used to speed up aluminosilicate solubilization for the development of the material's cementing characteristics [14]. Similarly, geopolymer can also be defined as either pure inorganic or organic alkaline-solution substance with a high silica and alumina content, according to Kim et al. [15]. These materials resemble zeolite with a polymeric Si-O-Al framework and their binding properties depend on $SiO_2/Al_2O_3$ ratio in the framework. In recent decades, this group of minerals has become one of the most important substitutes for conventional cement (OPC) as a binder for the manufacture of pre-cast concrete. This is due to their respectable durability qualities like low shrinkage, fire resistance, acid resistance and environmentally sustainable for the construction industry [16–20]. They are environmentally friendly materials since they have low manufacturing temperature and $CO_2$ emission which is estimated to be nine times less compared with OPC [16]. The demand for long-established natural raw materials and aggregates in cement as a binder and concrete is greatly brought to a minimal level by the use of industrial by-products in the creation of geopolymers. This directly reduces $CO_2$ emissions, landfilling, and energy consumption as well [21, 22]. As a result, it has proved to be a "green material," meaning that it utilizes little energy during manufacturing and emits little waste gases [23]. Due to this, geopolymer is now one of the contenders for resolving the conflict between societal growth and environmental pollution caused by the production of binders [24]. Therefore, geopolymer has applications in waste management, biomaterials, fireproofing, building engineering, and other fields [25, 26].

In comparison to PC, processing geopolymer cement uses less fuel, less calcium-based raw material, and lower manufacturing temperatures. As much as 80% to 90% less carbon dioxide is released as a result [16]. Aluminosilicate AAMs are used to create geopolymers, which can have stronger final products and do so more affordably than OPC [18]. Typically, the first four hours of the setting are when 70% of the final compressive strength is reached [27]. Geopolymer constructions exhibit decreased permeability, resilience to fire and acid attack, better unconfined compressive strength, significantly less shrinkage, excellent heavy metal ion solidification, and exceptional freeze-thaw cycle resistance. It's considered a high-strength concrete application that demonstrates strong resistance to fire, acid, and/or chloride penetration. So, for the chemical and nuclear sectors, geopolymers may offer a promising waste immobilization solution.

The favorable effect of geopolymers on the durability performance of the resulting cementitious composite is their principal benefit. This is connected to their dimensional stability, especially with geopolymer compositions that have very low C-S-H levels [28]. The primary reaction occurs when amorphous aluminosilicates in metakaolin-based materials and other amorphous aluminosilicate materials, such as fly ash and volcanic ash with low calcium concentrations, are activated by alkalis. In essence, this causes the creation of polysialates (M-A-S-H). The attack of alkali on aggregates is the secondary reaction, although, in the absence of calcium, this won't have much.

The nature and composition of the reaction products produced by geopolymers or alkali-activated cementitious materials typically rely on the type of agro-industrial by-product of the aluminosilicate precursor used, and they differ from those normally derived from OPC. The production of each of these compounds depends on the Ca/Si and Si/Al and the pH contents of the matrix. For hybrid cementitious materials, Garcia-Lodeiro et al. [29], documented the existence of several gels. This included calcium silicate hydrate (C-S-H) from the usual hydration of PC, calcium aluminosilicate hydrate (C-A-S-H), and (N, C)-A-S-H gels, which are the main by-products of the alkaline activation of aluminosilicate. In comparison to the same type of cement without activation, Palomo et al. [30], found a 50% improvement in strength at an early curing age, a lower heat of hydration, and an early setting time. They explained this as being caused by the availability of C-A-S-H, N-A-S-H, and (N, C)-A-S-H gels, which have previously been noted from hybrid types of cement made of 7:3 of FA: OPC [31].

The alkali-activated gel is created as a result of the exothermic reaction between solid aluminosilicates and hydroxide, silicate, and sulfate solutions of alkali, which promotes the ions dissolution of both $Al^{+3}$ and $Si^{+4}$ from starting materials [32, 33]. This gel exhibits high-quality mechanical and durable properties in the hardened phase.

Geopolymer cement can be classified as fly ash, slag, rock, or ferro-sialate-based geopolymer types of cement. Alkali-activated binder, an inorganic polymer, mineral polymer, hydro ceramics, and alkali-bonded ceramic are some further names for this substance [34, 35]. Substituting waste for Portland cement in the industrial manufacturing of activated alkali materials or geopolymer binders will have positive economic and environmental effects. It would also resolve the issues related to the removal of significant amounts of garbage from industry and building sites that could otherwise threaten the environment, such as coconut shells and calcined clay brick waste.

## 2. RAW MATERIALS FOR GEOPOLYMER SYNTHESIS

In addition to the alkaline solution, silica-aluminum sources are used as raw ingredients in the production of geopolymer concrete. For the synthesis of geopolymers, there are two types of raw materials. Along with the alkaline activating solution, which is often an alkali metal hydroxide or silicate solution, this also includes the reactive aluminosilicate particles such as fly ash and calcined clays. One-part geopolymer precursors have generated interest [36–38] however, the strength of the materials do not match the requirements for the majority of construction applications. Different aluminosilicate industrial waste materials have traditionally been shown to pose effective options for the synthesis of geopolymer. These include building demolition debris, metallurgical slag, coal fly ash, and a variety of biomass ashes like rice husk ash, coconut shell ash, palm oil fuel ash, and others [39, 40]. The two most often used starting materials in the synthesis of geopolymers for use in the building are fly ash and calcined clay. Industrial waste or by-product created during the production of coal-fired energy is called fly ash [41]. For geopolymers production, a wide range of raw materials with high silica and alumina contents can be employed. Depending on where they come from, the raw materials are categorized into three classes. Among them are primary raw materials, which are composed of natural minerals and secondary raw materials, which are industrial by-products and their wastes and by-products raw materials of natural origin [42].

Natural minerals from the earth's crust, which comprises 65% Al-Si elements, are the main suppliers of raw materials [23, 43]. Several Al-Si minerals and clays, primarily kaolinite and metakaolin, have been found to polymerize in the past [23]. A purer and easily described starting material for geopolymerization is provided by metakaolin. Due to its predictable qualities and stable chemical make-up, it is also commonly employed for industrial and scientific applications. Poorly activated kaolin produces geopolymers based on metakaolin, which are too soft and water-intensive to be of much use in building applications [44–47]. The reactivity of kaolin can be improved by either mechanical or thermal treatment. Mechanical activation involving prolonged grinding decreases the degree of crystallinity and surface energy and hence increases the chemical reactivity [48]. Dehydroxylation of kaolinite at 600–800 °C for 2–5 hours results in metakaolin [44, 47], depending on purity and crystallinity, as shown in Equation (1).

$$Al_2O_3.2SiO_2.2H_2O \dashrightarrow Al_2O_3.2SiO_2 + 2H_2O \quad (1)$$

Metakaolin is a highly reactive anhydrous aluminosilicate-metastable clay that can be produced by calcining kaolin to temperatures between 650 °C and 700 °C, according to [49, 50]. According to earlier studies, the reactivity of metakaolin changes as a result of heat treatment at calcination temperatures between 450 and 600 °C [51, 52]. According to [53] Table 1 displays the normal chemical composition of metakaolin.

**Table 1.** Typical chemical composition of metakaolin

| Chemical compounds | wt % |
|---|---|
| $SiO_2$ | 55.62 |
| $Al_2O_3$ | 39.67 |
| $Fe_2O_3$ | 0.96 |
| CaO | 1.41 |
| MgO | 0.18 |
| $K_2O$ | 0.87 |
| $SO_3$ | 0.00 |
| $TiO_2$ | 0.41 |
| $Na_2O$ | 0.08 |
| LOI | 2.01 |

Burnt clays' ability to acquire pozzolanic properties is influenced by the raw material's quantity and kind of clay minerals present, the calcination conditions, and the fineness of the finished product [54–57].

Wastes and by-products from industry are secondary raw resources. The secondary raw materials are used in making more environmentally friendly geopolymers which also help in preserving natural resources [58, 59]. These include waste broken bricks, waste glass, fly ash, red mud, and blast furnace slag [60, 61]. Fly ash and slag are the secondary raw materials that are used and studied the most [42]. Fly ash and blast furnace slag are examples of secondary raw materials that are heterogeneous and contain contaminants like calcium and iron. This opens up more chemical pathways during polymerization, which may have an impact on the final product's setting times, slump, strength, and shrinkage [19, 62, 63].

Fly ash which is a by-product of power plants fueled using coal, mostly consists of $SiO_2$ and $Al_2O_3$, along with a few minor substances like CaO, $Fe_2O_3$, MgO, etc. Since it has high alumino-silicate, better workability, low water demand and readily available thus has been a material of concern for geopolymer synthesis. Geopolymerisation of fly ash with alkaline media forms a cementitious material that comprises of alumino-silicate-hydrate (A-S-H) gel [64]. This geopolymer product has improved durability and strong mechanical strength [65]. However, the low reactivity of the material has limited the manufacture of geopolymers by delaying early setting and strength development [64]. Studies in microscopy and microanalysis of residual fly ash particles found in geopolymer cement show that mullite available in fly ash remains unreacted and that calcium appears to be active in the process of alkali activation of fly ash blends [66, 67].

Cooling quickly the molten iron slag from a blast furnace in water or steam, a glassy granular material known as granulated blast furnace slag (GBFS) is produced. This is usual-

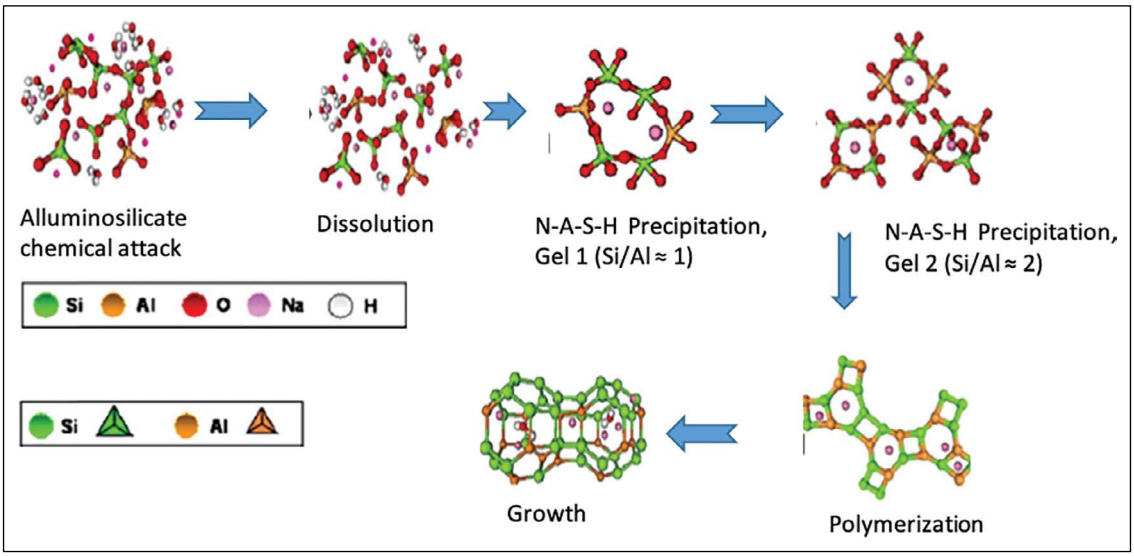


**Figure 1**. Geopolymerization process [82, 81].

ly very reactive with a mineral composition of $SiO_2$, CaO, $Al_2O_3$ and MgO [42, 67, 68]. Due to its small particles, it has effectively increased its strength. As a result, GBFS has been used as a replacement material for making cement for over 75 years [19, 67–69]. A hydrated calcium-silicate (C-S-H) gel with a low C/S ratio is produced as the main reaction product during the alkali activation of GBFS. The strength and setting properties of the geopolymer are enhanced by this gel [70–72]. Hadi et al. [72], worked on a blend of GBFS with fly ash (FA), metakaolin (MK) and silica fume (SF) in nine mix designs. Their formulations gave a better early 7-day compressive strength and setting time compared to conventional cement. In another investigation on the effect of curing conditions on the performance of granulated blast furnace slag and metakaolin-based geopolymer concrete, it was concluded that the use of the GBFS/MK reported good mechanical performance degradation [73].

Red mud is another industrial waste produced during the extraction of alumina from bauxite ores. It mainly consists of $Al_2O_3$, $SiO_2$, and NaOH [74]. It is suitable for the synthesis of geopolymers owing to its high alkalinity as well as the presence of alumina [75]. Since its silica component is non-reactive, it is typically utilized in conjunction with other alumino-silicate compounds like fly ash or metakaolin. Roadway building using red mud geopolymers may be a viable option for cementitious materials, helping to lessen the harm that waste has on the environment and human health [16, 76]. Due to its density and resistance to ion penetration, red mud-blast furnace slag geopolymer mortar was found by Liang & Ji [77] to be more durable than PC mortar in terms of protecting steel bars from corrosion. Substitution of 10–15% red mud to alkali-activated fly ash, improved the compressive strength increased by 2.5 times. This was linked to changes in phase composition and activator ratio which inhibits zeolite formation [78].

Wastes and by-products of mineral origin are natural by-products that are produced during the manufacturing process from raw materials. Perlite is an amorphous volcanic glass that contains some crystalline phases and is high in $SiO_2$ and $Al_2O_3$. It is reduced in size and heated to create a porous product, which is then used as an agricultural water-absorbent [42, 79]. The perlite that is too fine or has an insufficient ultimate porosity, for example, to be used further, is regarded as trash. Waste perlite that has been geopolymerized, can be utilized to make effective thermally insulating materials, or it can be combined with fly ash or other waste aluminosilicates to make building materials and immobilize hazardous waste [80]. A study by Vance et al. [79], on the use of perlite waste in the preparation of geopolymer, reported that perlite waste in small particles acted as a fairly reactive aluminosilicate constituent with a strong alkali solution in geopolymer formation. Vaou & Panias [80] investigated the foamy geopolymers from perlite. They found that this material had very good thermal insulation and compressive strength of 780 kPa at 2% deformation and a fracture behavior resembling one of the rocks. In addition, it had high fire-resistant properties.

## 3. MECHANISM OF GEOPOLYMER SYNTHESIS

According to research, the geopolymerization process involves three steps: (1) using an alkaline solution to dissolve (2) diffusion and ion reorganization along with the formation of minute coagulated structures; and (3) soluble species are polycondensed to create hydrated products [18, 81]. The Figure 1 illustrates the geopolymerisation process.

The amorphous, zeolite-like geopolymers are created by the high-pH dissolution of silica- and alumina-containing parent materials. Aluminosilicate raw materials containing $Si_2O_3$ and $Al_2O_3$ (or other compatible Metal Oxides such as

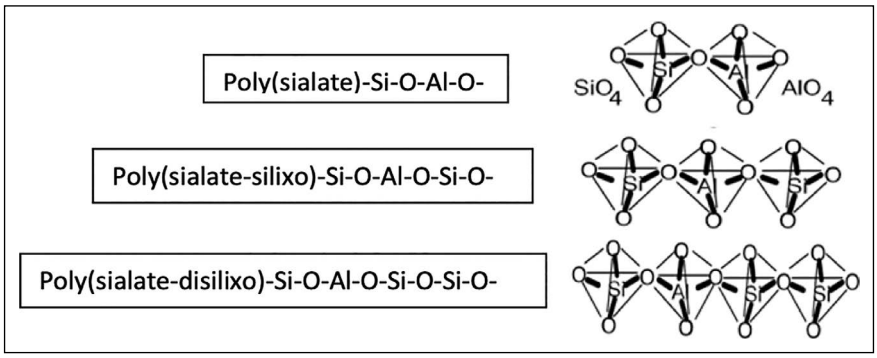


**Figure 2**. The fundamental process by which various alumino and silicate species co-polymerize to form polysialate.

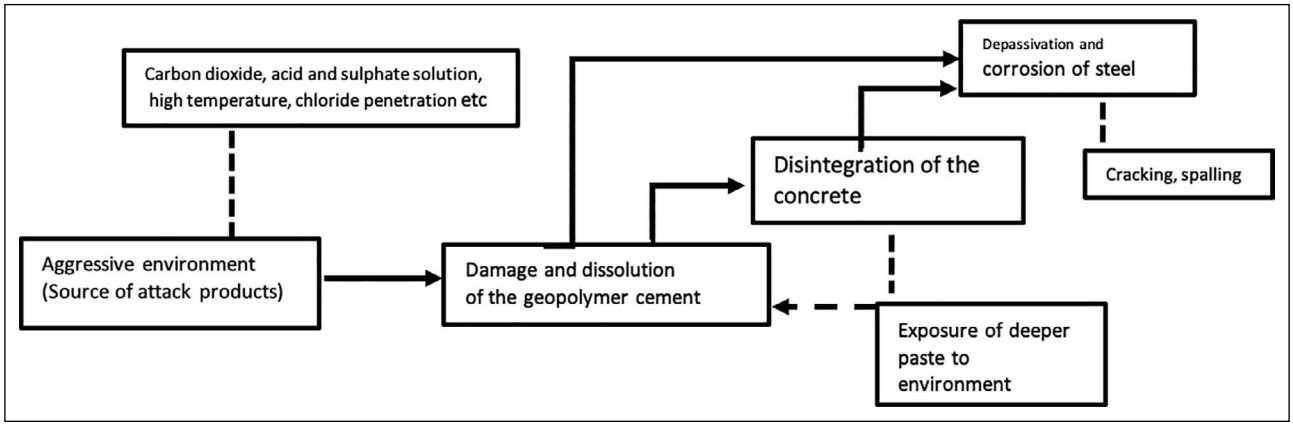


**Figure 3**. Cement/geopolymer concrete's general mechanism for deterioration [95].

$Fe_2O_3$) are reacted with a soluble alkali such as K or Na. The $Si_2O_3$ and $Al_2O_3$ oxides undergo dissolution into atoms forming a gel. The free atoms within the gel move, forming monomers that form polymers and oligomers. The latter forms 3-dimensional chain networks if the correct ratio of Si: Al is present within the mix expelling water to form the bond, i.e. dehydroxylation. The polymeric bonding continues until a solid hardened structure emerges [83]. Dissolution of these leads to co-polymerization of individual alumino and silicate species [27, 84, 85] to form silico-aluminates i.e poly(sialate). According to Figure 2, Poly (sialates), which can be amorphous or semi-crystalline and feature $Si^{4+}$ and $Al^{3+}$ in IV-fold coordination with oxygen, are chain and ring polymers.

To create the sialate network, $AlO_4$ and $SiO_4$ tetrahedra are linked alternately by sharing all of the oxygens. The framework cavities contain positive ions, such as $Na^+$, $K^+$, $Ca^{2+}$, Li+, $Ba^{2+}$, $NH^{4+}$, or $H_3O^+$ to counteract the negative charge of Al3+ in IV-fold coordination. The written empirical formula for poly(sialates); $M_X\{(SiO_2)_ZAlO_2\}_xwH_2O$.

Where, Z is 1, 2, 3.., M is a cation like calcium, sodium, or potassium and x is a polycondensation degree [86]. Geopolymerisation is an exothermic process and involves polycondensation of orthosialate ion monomers as in Equations (2) and (3).

$$n(Si_2O_5Al_2O_2) + 2nSiO_2 + 4nH_2O \xrightarrow{NaOH/KOH} n(OH)_3\text{-}Si\text{-}O\text{-}Al(OH)_2\text{-}O\text{-}Si\text{-}(OH)_3 \quad (2)$$

$$n(OH)_3\text{-}Si\text{-}O\text{-}Al(OH)_2\text{-}O\text{-}Si\text{-}(OH)_3 \xrightarrow{NaOH/KOH} (Na/K)\text{-}(\text{-}Si\text{-}O\text{-}Al(O)_2\text{-}O\text{-}Si\text{-}O\text{-}) + 4nH_2O \quad (3)$$

## 4. DURABILITY ASPECTS OF GEOPOLYMERS

Alumino-silicate waste can be geopolymerized to provide a variety of mining and construction materials with superior chemical and physical qualities. These characteristics include resistance to fire, chemical stability, acidity, salts such as chlorides and sulfates [40, 87] resistance to humidity or water, freezing action, and weathering [88–90]. The stability and durability characteristics of geopolymers are similar to those of more conventional cements like Portland or blast furnace cement since they have an alkaline nature [91, 92]. Durability is a crucial factor since it measures a material's capacity to operate both temporarily and permanently despite abrasion, chemical attack, and weathering while retaining the necessary qualities [93, 94]. To understand the geopolymers' chemical reactions when exposed

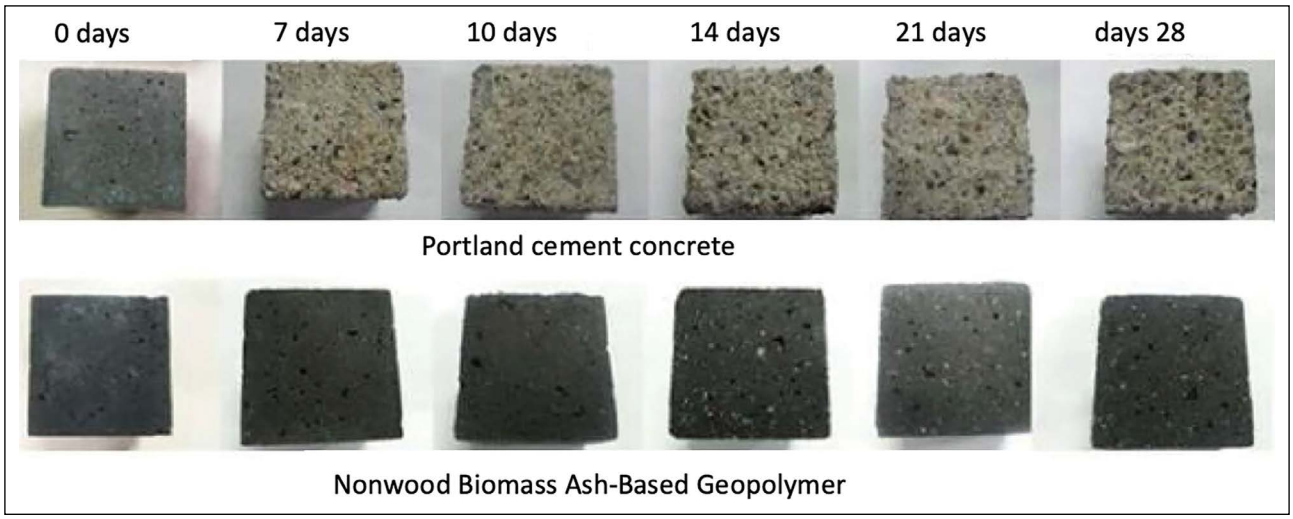


**Figure 4**. Visual characteristics of non-wood biomass ash-based geopolymer in acid attack on ordinary Portland cement concrete [98].

to aggressive substances, it is required to investigate their durability properties. When materials' compositions alter, the geopolymer degrades, and the paste dissolves and deteriorates when it is exposed to aggressive environments [95], as seen in Figure 3.

### 4.1. Acid Attack

Cementitious materials are susceptible to reaction with acidic chemicals in a range of applications, including effluents, sewage treatment facilities, power plants, agriculture and in addition to transportation and raw material storage facilities [96]. One of the qualities that building materials should have is resistance to acidic environments. Such an acidic environment can be a result of acid groundwater, acid rain, the acid solution from the sanitary sewer, animal feed and manure, waste stabilization applications, chemical and mining industries [91, 97]. OPC and geopolymer binders are acid attack-prone due to their alkaline nature. As pH decreases, calcium hydroxide and calcium sulfoaluminates breakdown first in the case of PC binder, then C-S-H decalcifies. The hydrated PC paste's main C-S-H component has a comparatively high Ca to Si ratio, leaving a porous structure on its outer layers that is vulnerable to further acid attacks. The typical alkaline earth or alkali aluminosilicate hydrate polymeric binder component, on the other hand, forms a thick silica gel protective layer on its outermost layer in an acidic environment. This slows down additional acid attacks, giving geopolymer binders a better acid attack than PC binders. Matalkah et al. [98], used visual comparisons to contrast normal PC cement concrete concrete specimens with nonwood biomass ash-based geopolymer concrete specimens that were immersed in 5% sulfuric acid solutions for up to 28 days. Figures 4 and 5 show that the PC concrete exhibited significant surface degradation and mass loss in comparison to geopolymer concrete made of

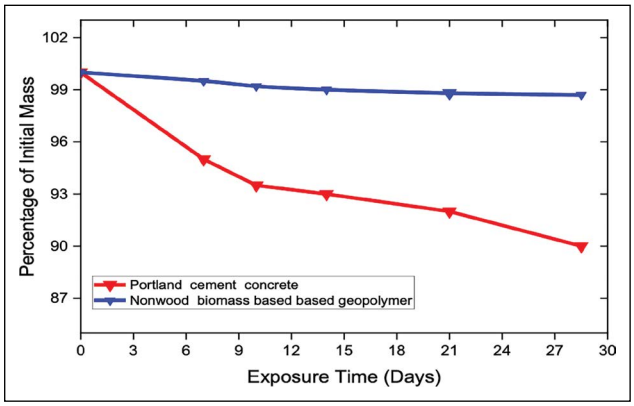


**Figure 5**. Mass measured against time immersed in acidic solution [98].

nonwood biomass ash. They attributed this to the geopolymer's nonwood biomass ash base's stable chemistry and good barrier properties.

On geopolymer made from palm oil fuel ash, metakaolin or calcined kaolin, fly ash, bottom ash, rice husk ash and slag studies of acid resistance have previously been conducted [99–104]. The method of acid attack varies depending on the type of acid and the characteristics of the calcium salt generated, according to [105]. The structural integrity of the geopolymers will also depend on the dissociation of the cations in either the alkali or acid environments. For instance, the precursor material's iron compounds are prone to acid degradation since they play a little role in the geopolymerization procedure and may dissolve leaving pores [106]. The amorphous aluminosilicate spheres are vulnerable to both alkali and acid damage when left unreacted. This is because Al dissolves more in acids than Si. Also, both Al and Si disintegrate in alkali with Si having the highest solubility. Thus, the amount of amorphous precursor materials

in the geopolymers determines the alkaline or acid resistance behavior. The amorphous compounds have generally a weaker resistance to chemical attack compared to their crystalline counterparts [97].

Conventional concrete constructed with OPC does not offer acid resistance. Alkali-activated or geopolymer concrete has also started to gain favor as most researchers work toward sustainable development because research has proven that it is stronger and more durable than regular concrete [72]. The cementitious materials acid resistance is affected by the concrete matrix's impermeability and the strength-forming phases' resistance [107]. Several approaches have been used to improve the impermeability of the concrete matrix such as the decrease in w/c ratio with minimal impact. According to research, creating a more stable phase is the greatest way to increase acid resistance. For instance, lowering the amount of clinker in Portland cement-based binders by using supplementary materials like metakaolin results in a decrease in the acid-soluble $Ca(OH)_2$. This also leads to the formation of C-A-S-H -phases with lower C/S ratios, hence low leaching property [107, 108]. CASH phases offer more acid resistance than regular CSH phases made from other pozzolanas, such as fly ash.

Working on the acid corrosion resistance of various cementing materials, Shi & Stegemann [109], proposed that the permeability of hardened cement pastes was less important for cement paste resistance to acidic corrosion than the composition of the hydration products. Alkali-activated blast furnace slag cement, lime, and fly ash paste primary hydration product was C-S-H with a low C/S ratio, whereas hardened PC paste primary hydration products was C-S-H with a high C/S ratio and $Ca(OH)_2$. Acid exposure had a deleterious effect on the latter, hardened mortar [109]. As a result of sulphuric acid attack, cementitious phases in the matrix disintegrate and decalcify and sulphate salts crystallize on the exposed surface [110, 111]. This affects both the mechanical and physical characteristics of the concrete, including its porosity and strength, in addition to its density [110, 112]. These alterations in the matrix allow acid to permeate deeper into the concrete layers and neutralize them.

Geopolymer concretes have the potential to replace ordinary PC concrete in construction sites exposed to an aggressive environment [113]. The aluminosilicate secondary raw materials, such as metakaolin, fly ash, and ground granulated blast-furnace slag (GGBS), react with an alkaline activator comprised of metal hydroxide or silicate solution to produce the binders. Highly cross-linked alkali-aluminosilicate is created during the alkali reaction with aluminosilicate and is referred to as geopolymer [114, 115]. The microstructure is made of a three-dimensional network of randomly connected negatively charged $(AlO_4)^{-5}$ and $(SiO_4)^{-4}$ tetrahedrons that are balanced by cation M+ ($K^+$ or $Na^+$). Geopolymer binder formed from low calcium aluminosilicate precursor and sodium silicate or hydroxide solutions as an alkaline activator has shown to form an amorphous form of N-A-S-H gel which has shown resilience to an acidic environment [99]. As seen in equation 4, the disintegration of this amorphous gel matrix caused by the liberation and substitution of a proton (H+) with an alkali cation (M+) is what gives geopolymer its chemical resistance.

$$[\text{Si-O-Al-O}\ldots]\text{H+ M}^+ \rightarrow [\text{Si-O-Al-O}\ldots]\text{M+ H}^+ \quad (4)$$

This occurs following the breakdown of the Si-O-Al network and the elimination of alumina. This Al delinking from the aluminosilicate structure results in the formation of Si vacancies, which when combined form an unfinished weak silicic acid [99].

Alkali-activated binders have in recent times shown resilience against aggressive environments like hydrochloric acid, sulphate, sulphuric acid, nitric acid, or acetic acid [97, 116–119]. This contradicts the observation by Lloyd et al. [118], that acid attacks inorganic polymer binders by surface corrosion. Deterioration of inorganic polymer binders is well tested by corroded depth instead of a change in mass. This is because the extremely interconnected aluminosilicate bonds of an inorganic polymer binder are attacked by acid. Instead of wearing away, as has been the case for other binder types, this causes the creation of a physically unstable and porous but intact layer on the sample surface [118].

Acidic corrosion known as nitric acid attack reduces the volume of the damaged layer as a result of the creation of the extremely soluble calcium nitrate salt [120]. According to Thokchom et al. [121], three different specimens made by alkali initializing fly ash with a mixture containing sodium hydroxide and sodium silicate solution containing sodium hydroxide from 5% to 8% of fly ash were tested for the durability of fly ash-based geopolymer mortar samples in nitric acid solution. The researchers submerged samples in a 10% weight solution of nitric acid for 24 weeks. Analyses were carried out in terms of overall aspect, weight change, and compressive strength change. Adjustments in mineralogy and micro-structural caused by nitric acid threat were also investigated. Geopolymer mortar specimens demonstrated outstanding durability in aspects of relatively low weight loss and high compressive strength retention. Also, specimens with a greater alkali content were more resistant to nitric acid.

Previous analysis indicates that geopolymer mortars outperform ordinary Portland cement mortars in terms of sulfuric acid resistance, with lower shrinkage and reduced compressive strength. Similar patterns were seen by Purbasari et al. [122], who studied the resilience and microstructure of geopolymer mortars formed from co-combustion residues of bamboo and kaolin after being subjected to a solution of sulfuric acid at 5% for 2, 4, and 6 weeks. The researchers discovered that when compared to conventional Portland cement mortars, geopolymer mortars

had superior sulfuric acid resistance in terms of lower mass and compressive strength loss. When subjected to a 2% sulphuric acid solution for up to 45 days [123], investigated the durability of geopolymer concrete made with high calcium fly ash and alkaline activators. The findings demonstrated a compressive strength drop of 20% and 28% in the geopolymer concrete and the conventional Portland cement concrete respectively. Song et al. [124], conducted an experiment to see how long concrete made with fly ash will last when exposed to 10% sulfuric acid solutions. With an evaporation rate of less than 3%, the study demonstrated the remarkable sulphuric acid resistance of geopolymer concrete. Furthermore, the Geopolymer cubes were structurally sound and still had a sizable load capacity even after the entire portion had been neutralized by sulfuric acid. Geopolymer concrete subjected to acid and salt was examined for strength by Kumaravel & Girija [125]. The workers claimed that the GPC specimens exhibited outstanding resistance to acid and salt, with a little higher concentration of NaOH as alkali, or 12 M.

The strongest leaching and subsequent quick loss of thickness are caused by citric acid, which has proven to be the most aggressive of all organic acids [126]. Citric acid's polyacidity and the precipitate's lack of protective qualities may be to blame for this. The solubility and acid buffering properties of the organic salts may potentially contribute to the increased harmful effect [127]. Acetic acids found in effluents and damping sites can be aggressive as an acid attack. At equivalent concentrations, the corrosion process is comparable to that of strong acids such as sulphuric acid but less aggressive than that of citric acid [105]. Ukrainczyk et al. [128], did a degradation comparison of GP, Calcium Aluminate and OPC mortar on acetic acid. The results showed that GP concrete was least affected by the exposure to the acetic acid in terms of mass loss, hardness, and porosity. The workers attributed this to the strong aluminosilicate network structure of GP which remains stable after the leaching of alkali ions. The penetrating acid species are highly soluble in the OPC binder phases such as CH, C-S-H, AFt, and AFm, creating a very porous binder matrix. As a result, geopolymer-based mortars have better acid resistance and may be a viable substitute for conventional cement concretes used in a variety of agro-industrial settings.

### 4.2. Chemical Attack

#### *4.2.1. Sulphate Attack*

The long-term endurance of a concrete structure may be threatened by salts and solutions of sulphate-bearing chemicals found in saltwater, industrial water effluents, groundwater, or soils nearby [129]. Depending on the calcium level, geopolymers in a sulphate environment erode in different ways [130, 131]. High calcium alkali-activated systems have similar eroding mechanisms to OPC because hydration products resemble each other [95]. The form and extent of damage to concrete will depend on the sulphate concentration, the type of cation (e.g $Na^+$ or $Mg2^+$) in the sulphate solution, the pH of the solution, and the microstructure of the hardened cement matrix. Gypsum ($CaSO_4.2H_2O$), ettringite ($[Ca_3Al(OH)_612H_2O]_2(SO_4)_32H_2O$), or thaumasite ($[Ca_3[Si(OH)_612H_2O](CO_3)SO_4$) or mixes of these phases are precipitated as a result of sulfate ions' reaction with the pore [132, 133]. These solid phases' precipitation may cause tension within the material, which may result in expansion, strength loss, spalling, and severe degradation [54]. Calcium hydroxide (CH) consumption lowers pH, which can eventually cause the C-S-H to become decalcified. When the magnesium sulfate solution directly attacks the C-S-H, non-cementious M-S-H is formed [134].

When geopolymer/AAM with little to no calcium content is attacked by sulfate, there typically is an exchange of cations with the sulfate solution. This leads to the formation of N-A-S-H, a less expansive crystalline phase structure hence more resistant to sulfate attack [131]. Geopolymer mortars outperformed Portland cement mortars in terms of durability when exposed to magnesium sulfate solution, according to studies by [135] on Magnesium sulfate resistance. This phenomenon is attributed to the higher amounts of $Ca(OH)_2$ and $C_3A$ in OPC thereby producing gypsum on the attack by sulphate ions (Equation 5). Moreover, calcium silicate hydrate abundant in OPC reacts with sulfuric acid to form $SiO_2$ in an aqueous state weakening the structure's strength (Equation 6).

$$Ca(OH)_2 + SO_4^{2-} \rightarrow CaSO_4 2H_2O \quad (5)$$

$$CaO.SiO_2 + xH_2SO_4 + xH_2O \rightarrow xCaSO_4 2H_2O + SiO_2 \quad (6)$$

The "sulfate attacking" process that occurs on geopolymer binders is significantly influenced by the cation that the sulfate is connected with [136]. According to research by Ismail et al. [137], it is important to distinguish between "magnesium sulfate attack and broader processes connected to the presence of sulfate along with other, non-damaging cations. It is important to note that both $Mg^{2+}$ and $SO_4^{2-}$ are capable of causing damage to a cement structure. The fly ash/slag binders investigated here were more unfavorable in $MgSO_4$ than $Na_2SO_4$, though not by as much. This was related to the earlier situation's development of calcium sulfate (gypsum), which expanded and damaged the material [138].

In a study by Albitar et al. [139], geopolymer concrete durability parameters were studied against OPC by immersing mortar cylinders into solutions containing 5% sodium chloride, 5% sodium sulfate, and 5% sodium sulfate + 5% magnesium sulfate and 3% sulfuric acid solutions for 9 months. To investigate the effect of chemical conditions on the durability of the concrete, the authors reported that the geopolymer concrete was most resilient to sulfuric at-

tack. This phenomenon is attributed to the higher amounts of $Ca(OH)_2$ and $C_3A$ in OPC thereby producing gypsum on the attack by sulphuric (Equation 5). Moreover, calcium silicate hydrate abundant in OPC reacts with sulfuric acid to form $SiO_2$ in an aqueous state weakening the structure's strength (Equations 5 & 6).

Gupta et al. [140], demonstrated a similar resistance of geopolymer concrete to acid attack in a subsequent study examining the mechanical and durability characteristics of a geopolymer composite made of slag and calcined clay. The researchers studied performance at 7, 28 and 56 days using 5% sulfuric and 5% magnesium sulfate. Water permeability was however lower in geopolymer concrete than in conventional, a disagreement with findings by Albitar et al. [139]. This was so probably due to the difference in experimental designs.

Concerns have often arisen concerning the effectiveness of geopolymer concrete modifications due to the uncertainty surrounding this process. Chithambar et al. [138], worked on the durability of fiber-reinforced geopolymer concrete against chloride penetration, sulfuric acid attack, and hydrochloric acid attack among other tests. The geopolymer used in the study was synthesized using M-sand and sodium hydroxide and silicate. The effect of glass and polypropylene fiber on the performance of the concrete was studied. Chloride resistance was reported to increase with polypropylene fiber reinforcement. The reinforced concrete also showed high resistance to acid and sulfate attacks.

According to investigations on geopolymer mortar made of fly-ash produced with various alkali content by Thokchom et al. [121] and Thokchom et al. [141] exhibited variable degrees of degradation when exposed to sulfuric acid. Using an optical microscope, the results showed deterioration of mortar surface with advanced effects on specimens with lesser alkali content.

#### *4.2.2. Chloride Attack Resistance*

Attack on the reinforcing steel by chlorides is the most frequent cause of durability failure in reinforced concrete (RC) structures. It adversely affects the service life of an RC structure as a result of effects including reduced steel cross-section, cracking, delamination, and spalling [142]. Therefore, the need to prevent steel corrosion is an important objective in ensuring the durability of steel RC structures. Chloride ions may come from a component of the concrete matrix or an outside source, like saltwater or industrial wastewater. Chloride ions mostly enter concrete under the influence of permeability and porosity [143]. In other words, ions will penetrate pores more deeply the larger they are. The secondary precursor in AACs closes the pores, preventing chloride ions from entering the substance. Additionally, the C-A-S-H gel's dense and compact nature aids in the delayed transport of chloride into geopolymers, resulting in a greater chloride attack durability than OPC paste [144, 145].

The porosity of the geopolymer matrix determines how quickly chloride ions diffuse through it [146]. The precursor that has a larger surface area, along with a high concentration of amorphous silica and alumina, produces an aluminosilicate gel that is denser and less porous. This reduces the chloride ingress rate. Presence of CaO content influences the chloride binding capacity. This lowers the rate of chloride intrusion by causing chloride ions to adsorb on the gel's surface [147]. Ismail et al. [137], and Zhang et al. [148], working on fly ash-slag-based geopolymer found that the chloride binding depended mainly on physical adsorption. Other studies on geopolymer concrete performance against chemical attacks are summarized in Table 2.

### 4.3. Carbonation

When it comes to the major cause of concrete damage, as a result of steel corrosion, carbonation of concrete is regarded to be one of the most dangerous phenomena. Concrete suffers from the carbonation process because carbon dioxide diffuses through the pore structure and lowers the pH of the pore solution. Rapid destruction of the steel's passivation layer allows for unrestricted corrosion processes [155]. As a result of the internal expansion stress and weakening of the steel bars, structures eventually fail [87, 156].

When gaseous carbon dioxide enters partially wet concrete at a pH >10, a sequence of processes is often triggered. According to equations 8 and 9, it quickly dissociates into the alkaline pore solution before hydrolyzing to $HCO_3^-$ and $CO_3^{2-}$ ions.

$$CO_2 + OH^- \rightarrow HCO_3 \quad (8)$$

$$HCO_3^- \rightarrow CO_3^{2-} + H \quad (9)$$

At pore solution of pH 8, $CO_2$ hydrates directly forming carbonic acid ($H_2CO_3$) as shown in equation (10).

$$CO_2 + H_2O \rightarrow H_2CO_3 \quad (10)$$

At a higher pH the carbonic acid normally dissociates into $HCO_3^-$ and $CO_3^{2-}$ ions [157]. To create $CO_3^{2-}$ ions may then attack calcium-containing phases, like CaOH, C-A-H and. C-S-H. The calcium carbonate precipitates into either calcite, aragonite, or vaterite crystal polymorphs, based on the internal concrete conditions and the existence of impurities or additives [158, 159]. Under normal circumstances, calcite is the polymorph that is the most stable. Attack of CSH normally happens probably where the quantity of $Ca(OH)_2$ is less especially in blended or geopolymer types of cement, as shown in Equation 11.

$$CaSiO_3H_2O + CO_2 \rightarrow 3CaCO_3 + SiO_2 + H_2O \quad (11)$$

**Table 2.** Summary of studies on geopolymer concrete performance against chemical attacks

| Precursor(s) | Activator(s) | Other concrete modifiers | Chemical environment | Period of exposure | Observations | Reference |
|---|---|---|---|---|---|---|
| Metakaolin and bottom ash | 8M Sodium hydroxide and sodium silicate | – | 5% magnesium sulphate | 28 days | • GPC concrete had no precipitation on surface<br>• GPC concrete demonstrated higher resistance to sulfate attack | [149] |
| | | | 2% sulfuric acid | 28 days | • No cracks on GPC concrete specimen surface<br>• There was low weight loss in GPC specimens compared to OPC<br>• GPC compressive strength was least affected by acid attack compared to OPC | |
| Rice husk ash and ultra-fine slag with corn cob ash | 8M Sodium hydroxide and sodium silicate | – | Chloride ion environment | 28 and 56 days | • Concrete was moderately resistant to chloride ingress | [150] |
| Class F fly ash | 12M Sodium hydroxide and sodium silicate | Oil palm trunk fiber | 5% sulfuric acid | 90 days | • No significant changes were visually observed, in weight and cross-section.<br>• The outer region color changed from dark grey to light grey (corroded). Intensity corresponded to fiber content | [151] |
| Granulated blast furnace slag and dolomite | Sodium hydroxide and sodium silicate | Steel fiber | 3% sulfuric acid | 180 days | • Compressive strength loss 5 times lower than OPC<br>• Weight loss 24 times lower than OPC<br>• Steel fiber does not affect the weight loss/strength | [152] |
| | | | 3% sodium sulfate | 180 days | • Weight loss 5 times lower than OPC<br>• Weight loss not affected by steel fiber | |
| | | | Saline water | 180 days | • Weight loss 9 times less than OPC<br>• Strength loss 2.6 times less than OPC<br>• Percentage loss in compressive strength reduced by 13-15% with 0.25–0.75% addition in steel fibers | |
| Class F fly ash | 10M Sodium hydroxide and sodium silicate | Granite waste as fine aggregate | 5% sulfuric acid | 28 days | • When replaced at 5, 10, and 15%, granite waste is favorable to GPC.<br>• Loss in mass and compressive strength was lower than control GPC (best at 20% replacement) | [153] |
| Granulated blast furnace slag | 8M–16M Sodium hydroxide and sodium silicate | – | 5% hydrochloric acid | 28, 56 and 90 days | • 16 M NaOH GPC showed the highest resistance compared to OPC in 28 days | [154] |
| | | | 5% sodium chloride | 28, 56 and 90 days | • 16M NaOH GPC showed the highest resistance compared to OPC at 28 days | |
| | | | 5% sulfuric acid | 28, 56 and 90 days | • 10M and 12M NaOH GPC performed best at 28 days | |
| | | | 5% magnesium sulfate | 28, 56 and 90 days | • 10M NaOH at 28, 56 and 90 days showed the best resistance to sulfate attack | |

This lowers the alkalinity in the cementitious matrix, which allows the corrosion of steel-reinforced bars to spread and affects the mechanical performance of the material. Thus, the durability of the concrete is compromised [160, 161]. On the hand, this attack may be beneficial depending on the time, the extent to which they occur and the environmental exposure [162].

The disparities in the hydrate phase assembly, pore solution chemistry, pore structure, and transport capabilities between geopolymer carbonation concrete and Portland cement (PC) carbonation are related to variations in the concretes' binder compositions, ages, and curing circumstances [163]. The concrete's saturation level and $CO_2$ partial pressure, which in turn depend on exposure factors such as temperature, relative humidity and the period of contact with water, are all factors in the carbonation mechanism and kinetics [164].

The depth of the $CO_2$ penetration into cement pastes or concrete at a given time is typically used to describe the materials' resistance to carbonation. This is dependent on the substance's ability to bind $CO_2$ as well as its porosity and pore size distribution [165]. OPC has shown better binding ability because of the high content of portlandite. In their study of alkali-activated mortars containing waste ceramic powder and GBFS only, Huseien et al. [166], found that increasing the replacement of GBFS with fly ash (FA), increased the carbonation depth. This was attributed to a larger concentration of FA geopolymer materials in the matrix, which resulted in the addition of pore structure as gel formation was constrained to a small amount of Ca, showing a higher permeability and porosity to water than in the control [167, 168].

Compared to geopolymer concrete, ordinary silicate concrete has a different microstructure. and it is impossible to use the tools for carbonation analysis on ordinary concrete. However, geopolymer concrete's carbonation-proof performance is not necessarily superior to that of regular concrete. Prisms of fly ash-based geopolymer concrete were cured in the air for 8 years before their durability test was done by [169]. To assess the effects of carbonation, durability, pore-size distribution, and permeation qualities, large specimens from GPC culverts were compared to standard PC concrete under the same exposure conditions. It was shown that OPC concrete had greater carbonation resistance than GPC. This was attributed to the mix composition or design and the material used in this study.

The curing temperature of geopolymer mortar has been shown to influence the carbonation resistance. The heat-cured GP concrete of HGPC showed greater alkali leaching resistance and stronger carbonation resistance in the wet-dry repeating scenario than the ambient air-cured GP concrete of AGPC. Li & Li. [170], used the test of accelerated carbonation at various intervals and on a wide range of GP mortars and GP concrete to investigate the carbonation depths. At room temperature curing, they observed that the carbonation resistance of GP concrete was lower than the convectional OPC concrete. Heat curing was one of the elements in this study that enhanced GP carbonation resistance, along with other aspects including precursor quantity and fineness, alkali concentration, W/C ratio, and use of retarder.

The alkali solution used to activate the geopolymerization affects the carbonation resistance. The alkali solution's strength and concentration considerably impact both the formation of C-A-S-H gels and the crystallinity of calcium carbonates after carbonation. According to the [171] report, the NaOH slag activated was found to be more carbonation resistant than the NaOH / $Na_2SiO_3$ slag activated.

It has recently been hypothesized that carbonation affects the porosity and pore size characteristics of GPC concrete [172] studied this phenomenon using three-dimensional thermal neutron tomography, as a conservative analysis technique. They confirmed that carbonation lowered GPC porosity by approximately 30% and pore regions were shifted to smaller regions. This could be associated with the deposition of carbonation reaction products ($CO_2$ reacting with alkaline hydroxides in the GPC matrix) onto the pores of the concrete. This improves the GPC durability properties as the lower porosity discourages chloride ingress, thereby sustaining strength and corrosion protection [173].

In their investigation to assess the performance of GPC in various exposure conditions, Pasupathy et al. [169], showed that the source material type can also affect the carbonation mechanism and alkalinity of geopolymers. This might be explained by CaO's accessibility in various precursors. In comparison to the GPC with a higher proportion of slag, the fly ash-based geopolymer displayed a lower initial pH value. It was discovered that GPC concrete had higher carbonation levels than OPC concrete in all three environmental situations. However, as the slag component in the geopolymer mix increased, the rate of carbonation decreased. In comparison to the GPC with a higher proportion of slag, the fly ash-based geopolymer displayed a lower initial pH value. The researchers concluded that as compared to OPC, geopolymer concrete is more vulnerable to corrosion and carbonation. Law et al. [174], studied the pH levels of pore water recovered from geopolymer mortar specimens that had undergone 5% rapid carbonation. They suggested a pH level of 11 to safeguard the reinforcing steel after carbonation. In a similar investigation, Li & Li. [175], looked into the connection between GPC's durability and carbonation resistance. The authors reported that the increase in blast furnace slag in the GPC matrix had a corresponding increase in carbonation resistance. Other factors considered in this study were the NaOH content, slag texture and activator solution to active filler ratio.

Calcium carbonate precipitation forms on the OPC concrete's surface as a result of carbonation. This raises the concrete matrix's internal porosity and creates a barrier to carbon dioxide diffusion [176]. Calcium carbonate precipitation in geopolymer may cause volume change because of its poor volumetric stability in the ambient environment thus cracking. Additionally, the rate of carbonation in OPC is lower than that in geopolymer concrete, which is related to a higher Ca/Si ratio in the CSH gel [95, 176]. Based on all these factors, OPC concrete experiences less carbonation-related strength loss compared to geopolymer concrete. According to Marcos-Meson et al. [177], after carbonization, which causes N-A-S-H gel to develop, the compressive strength of fly ash slag-based geopolymers drops linearly. Further, it has been found that after carbonation, the reaction extent and mechanical properties of geopolymer concretes have decreased [156, 178, 179]. Other findings in carbonation have been summarized in Table 3.

**4.4. Creep and Shrinkage**

Concrete creep and drying shrinkage prediction is still an important parameter in the concrete specification, and it's critical for the long-term durability and serviceability of concrete constructions [183, 184]. While creep refers to the distortion of hardened concrete caused by a steady load, drying shrinkage relates to the cured concrete's internal moisture loss [185, 186]. Most often, shrinkage is described as the volume change in a matrix's geometry brought on by the removal of water from its surface (plastic shrinkage) and the gelling up of the matrix (drying shrinkage). It's also the matrix of a binder's self-desiccation and carbonation of heavier molecules with lighter ones [187]. Non-autogenous shrinkage includes, among other things, thermal deformation, carbonation, shrinkage, drying shrinkage and creep shrinkage [188]. Drying shrinkage is the term used by other researchers to describe a macroscopic dimensional reduction of hardened binders brought on by the evaporation of water or moisture within the products' matrix. When samples are subjected to a certain relative humidity (RH) and ambient temperature, this type of deformation happens [189]. In a comparable situation, plastic shrinkage results from an imbalance in the moisture exchanges between a specimen surface and its surroundings [190].

A chemical reaction on the hydrated concrete, known as autogenous shrinkage, as well as the loss of water as the concrete dries, known as dry shrinkage, are the two main causes of early-age shrinkage of concrete in the hours and days after casting. Typically, autogenous shrinkage increases when the water-to-cement ratio declines for concretes with the same aggregate and binder types, meaning that strength increases and drying shrinkage reduces. Other factors known to influence both creep and drying shrinkage of cement systems include cement type, aggregate type and content, age, temperature, relative humidity of the surroundings, curing, age, and particle size [191].

For moist-cured concrete, the drying shrinkage values suggested in the ACI 209 committee's report shouldn't be more than 800 microstrains, and for steam-cured concrete, they should be between 730 and 788 microstrains [192]. Drying shrinkage causes cracking, and while this may not affect structural integrity, it may raise durability issues, making it one of the most detrimental features of cement concrete. Studies on many components of mixed content and engineering behavior of geopolymers (GP) systems, such as shrinkage and creep, have just lately started to be published. Hardjito & Rangan [193] discovered lower creep coefficient values in their investigation of medium strength GP concrete than the same grade of OPC concrete. These researchers also discovered that as the compressive strength of GP concrete increased, the specific creep dropped. This finding is consistent with traditional OPC concrete. Normal 50 to 60 MPa PC concrete often has particular creep values in the literature that range from 50 to 60 microstrain after one year, with this value decreasing for greater strength concrete. In high-volume performance fly ash concrete, the specific creep was in the range of 30 microstrains per MPa after a year, according to [194].

While the effects of curing on the mechanical properties of GP concrete have not yet been thoroughly established, it has been observed that the drying shrinkage stress of heat-cured concrete specimens is frequently lower than comparable values recorded for ambient-curing concrete [188]. This phenomenon was due to water that is generated during the chemical reaction process of ambient-cured GPs and then evaporates over time, resulting in high drying shrinkage strains, especially during the first two weeks. The engineering performance of GP binders has also been investigated with other material-related features, such as pore network distribution. In their analysis of the pore network distribution of GP binders, Duxson et al. [195] found that there are several clusters of pore diameters that are comparable to those reported in OPC systems. To analyze the basic creep behavior of GP concrete at an early age, this study used similar grade Portland cement concrete as a standard. The studies measured the drying shrinkage response of concrete specimens while assessing the influence of age and stress on real creep at an early age. The drying shrinkage rate was considerably high in the early ages of up to 28 days, according to [196] studies. This research work which was based on GPC based on FA or MK showed drying shrinkage rate decreases beyond this age. They also noted a decrease in drying shrinkage values with an increase in FA and MK contents in the GPC. This is related to the FA or MK enhancing the polymerization process to create high connectivity into the alkali-activated cement matrix. Prior investigations that enhanced the structure have validated the production of products like C-S-H, C-A-S-H, N-A-S-H, and CN-A-S-H [197]. Also, this was due to the decreased calcium content in the cement mix hence reducing the hy-

**Table 3.** Summary of carbonation finding

| Precursor | Activator | Standard used | $CO_2$ environment | Exposure period | pH | Observations | | Reference |
|---|---|---|---|---|---|---|---|---|
| | | | | | | Carbonation depth | Carbonation product | |
| Low calcium fly ash and granulated blast furnace slag | 12M sodium hydroxide +2Ms sodium silicate | AS 1012·9 | 3% accelerated carbon dioxide | 2, 4, 6 weeks | 10.9 | 25 mm | 17.4% $NaHCO_3$ in 2 weeks | [156] |
| | | | 1% accelerated carbon dioxide | 2, 4, 6 weeks | <10 | 2.13 | $Na_2CO_3.10H_2O$ in 6 weeks | |
| | | | Natural environment | 6 months | 10.76 | 3 mm | 29% $Na_2CO_3.10H_2O$ | |
| | | | | 18 months | 10.22 | 3 mm | | |
| Municipal solid waste incinerator bottom ash and granulated blast furnace slag | Sodium hydroxide (4.8M) and sodium silicate (2.7Ms) | GB /T50107 - 2010 | Accelerated 20% carbon dioxide environment, 20+2°C (Lean GPC) | 14 days | – | 15.53 mm | $NaHCO_3$ | [180] |
| | | | | 28 days | | 20.14 mm | | |
| | | | | 60 days | | 25.65 mm | | |
| | | | Accelerated 20% carbon dioxide environment, 20+2°C (Modified with 10% slaked lime) | 14 days | | 8.2% reduction | $NaHCO_3$ | |
| | | | | 28 days | | 7.1% reduction | | |
| | | | | 60 days | | 4.8% reduction | | |
| | | | Accelerated 20% carbon dioxide environment, 20+2°C (Modified with cement) | 14 days | | 37.7% reduction | $NaHCO_3$ | |
| | | | | 28 days | | 37.9% reduction | | |
| | | | | 60 days | | 39.8% reduction | | |
| Class F fly ash | Sodium hydroxide (8M) and sodium silicate | – | Natural environment (Atmospheric exposure conditions) | 8 years | 9.92–10.41 | 45 mm fully carbonated, 70 mm partially carbonated | $Na_2CO_3$ | [169] |
| Class F fly ash | Sodium hydroxide (8M) and sodium silicate | – | Natural environment (saline environment) | 6 years | <7.5 | 135 mm exposed, 90 mm covered | $Na_2CO_3$ | [181] |
| Class F fly ash | Sodium hydroxide (12M) and sodium silicate | BS EN 14630 | Natural saline environment | 28–120 days | – | Undetected | Undetected | [182] |

dration rate of alkali-activated concrete. Other researchers have shown similar results of GPC concrete exhibiting lower drying shrinkage with the standard sample concrete as well as decreasing dry shrinkage values with an increase in the replacement of alkali-activated concrete [91, 198].

The creep and shrinkage are highly dependent on the curing conditions to which the concrete is exposed GPC concrete can be heat cured or cured in ambient temperatures, practices that induce varying creep and shrinkage effects. To investigate the most suitable curing conditions for GPC Khan et al. [199], studied early age shrinkage and creep. Two GPC mixes were cured at temperatures between 60 °C to 90 °C and ambient temperature. Axial tension was applied to unreinforced dog bone specimens, and it was shown that the curing temperature and time had an impact on the GPC's tensile creep coefficient and shrinkage. High temperatures were related to low early age shrinkage and high tensile creep coefficient. This was in agreement with a study by Frayyeh & Kamil [200] who observed that autogenous shrinkage would further be improved by the use of hooked-end steel fibers. In their study, an increase in hooked-end steel fiber content in the matrix has a corresponding decrease in autogenous shrinkage and tensile creep. They also went further to explore this concept by studying the effect of different reinforcing fibers on the dry shrinkage of geopolymer concrete. They used steel, propylene and carbon fibers. It was reported that improvement was generally seen across all the fibers, but steel fibers showed the highest effect. This was so since metallic fibers are generally stiff and therefore improve the concrete's flexural strength. Non-metallic fibers have a larger surface area and can control plastic shrinkage as a result [201]. Alkaline-activated natural pozzolans geopolymer binder was studied by [202], who claimed that the product's shrinkage was influenced by the curing method and chemical make-up of the basic materials. They also mentioned a connection between shrinkage and the Si/Na ratio.

Another factor that directly influences the creep and shrinkage of GPC is the void structure, which represents the bleeding behavior of concrete. Nazari et al. [203] studied the concept of void distribution patterns and their contribution to strength development in both OPC and GPC. The researchers found a correlation between the bleeding rate of concrete to dry shrinkage and concluded that modification of the bleeding rate is a necessary step to reduce early cracking in hardened concrete. They investigated the effect of slag content on the bleeding rate and found that slag reverses the indirect effect of void volume on the strength development of concrete. Similar conclusions were drawn by Negahban et al. [204] who concluded that pore structure and the distribution of voids are functions of strength development. Other findings on creep and shrinkage have been summarized in Table 4.

**4.5. Thermal Performance**

The global building and construction industry are very concerned about the longevity of structures made of cement. Cement-based materials are certified to be structurally sound at room temperature. Each year, it is reported that dangerous flames devastate a large number of cement-based structures around the world, causing staggering financial damage. Hazardous fires that affect these structures are largely caused by residential fires and electrical problems. In dangerous fires, these materials are subjected to temperatures that can be destructive. Due to thermal impacts on pore water and products, high temperatures have an impact on the concrete/mortar matrix's physical and chemical properties. Hazardous fires, therefore, shorten the service life of structures made of cement [206, 207].

In recent decades, research has increasingly focused on issues related to building materials' thermal performance and fire resistance. Thermal stability is essential for ensuring that they are safe to use within a specific temperature range with OPC beginning to lose strength irreversibly at 200 °C [208]. This occurs as a result of the principal binding phases, CSH, Ca(OH), and other hydrated products, deteriorating and losing water. Despite this, Jeon et al. [209], found that the breakdown of $Ca(OH)_2$ did not result in a significant loss of strength. However, the main cause of OPC strength reduction is the expansion of lime after chilling.

In past years, there have been a lot of studies done on the thermal characteristic of geopolymers exposed to high heat or fire. Geopolymers, like OPC, lose strength when exposed to high temperatures. Despite this, they maintained a substantially higher binding strength at the temperature range tested. Rivera et al. [210], investigated the effect of elevated temperature on alkali-activated geopolymeric binders compared to portland cement-based binders. The alkali-activated geopolymer showed minimal damage after the temperature exposure of up to 565 °C.

Geopolymer weight decrease is associated with higher strength retention [184]. Geopolymer mortars with a high concentrated slag showed increased strength loss at high temperatures of 600 °C, owing to the decomposition of CSH phases. Despite this, all blended geopolymer mortars-maintained strength between 23 and 25 MPa after being exposed to 600 °C. Compared to geopolymer mortar, geopolymer concrete lost less weight but lost more strength as the temperature increased. The difference in the thermal increase in volume between coarse aggregates as well as binder and the decreased binder concentration in concrete to combat paste shrinkage lead to considerable microcracking. They stated that geopolymers outlast regular concrete and even some high-performance concrete in terms of heat endurance.

**Table 4.** Summary of shrinkage and creep finding

| Precursor | Activator | Modifier | Standard used | Cure conditions | Initial parameters | Shrinkage and creep | Notes | Reference |
|---|---|---|---|---|---|---|---|---|
| Fly ash, sodium promotor and sand | 10M NaOH and 2.5Ms $Na_2SiO_3$ | 1% 3mm polypropylene fiber | RILEM TC 107-CSP (creep strain tests) | 75°C for 24h (synthesis conditions) 25 °C, relative humidity 30% (ambient cure conditions) | Compressive = 55.1 MPa @ 28 days | Shrinkage = 0.0002 mm/mm, Creep = 0.0013 mm/mm | • To measure creep and shrinkage strains, 20% of the ultimate compressive force was applied. • Creep and shrinkage data were collected up to the 35th day. | [192] |
| | | 5% 3 mm polypropylene fiber | | | Compressive = 33.9 MPa @ 28 days | Shrinkage = 0.0005 mm/mm, Creep = 0.0007 mm/mm | | |
| | | 1% 18mm steel fiber | | | Compressive = 48.4 MPa @ 28 days | Shrinkage = 0.0009 mm/mm, Creep = 0.0021 mm/mm | | |
| | | Unmodified (plain GPC) | | | Compressive = 52.5 MPa @ 28 days | Shrinkage = 0.0006 mm/mm, Creep = 0.0015 mm/mm | | |
| Fly ash | 12M NaOH and 2.5Ms $NaSiO_3$ | 1 wt% carbon fiber | 24h at 75 °C | EN 12390-3:2009 (compressive strength) | Compressive loading rate 0.7MPa/s | Creep = 0.00065 mm/mm | 1. Creep test at 20% ultimate compressive strength | [188] |
| Fly ash, granulated blast furnace slag | NaOH and $NaSiO_3$ | – | 25 °C for 24h (ambient curing), 70 °C for 6h (Accelerated curing) | AS – 1379 | Compressive = 62 MPa (ambient), 56.5 MPa (accelerated) Flexural = 7.1 MPa Indirect Tensile =5.1 MPa | Shrinkage = 450 microstrains Creep coefficient = 1.87 | 2. There was no significant increment in creep after 56 days 3. Compressive, flexural and tensile data was at 28 days | [205] |

Furthermore, according to Jiang et al. [211], fly ash, geopolymers preserved strength up to 400 °C and grew stronger at temperatures above 400 °C. In alkali-activated fly ash, crystallization of thermally stable minerals such as sodalite and nepheline was found. XRD diffractograms of geopolymer samples mostly revealed crystalline phases of nepheline when exposed to high temperatures. The presence of thermally stable crystalline phases is critical for geopolymer structure thermal stability. In addition, the solidification of melted stages aided in the development of strength. OPC, on the other hand, maintained compressive strength up to 600 °C before rapidly deteriorating beyond that temperature due to moisture loss and $Ca(OH)_2$ breakdown. The transformation of amorphous aluminosilicates into a geopolymer structure was revealed to be strongly reliant on the geopolymer's compressive strength. The resistance of the material to high temperatures and burning was influenced by the Si/Al ratio and iron content in the fly ash. According to Wang et al. [144], metakaolin-fly ash-based geopolymers have a strength of 46 MPa at 1000 °C. The high-temperature performance was improved with the addition of electrical porcelain as aggregates. The thermal stability of potassium-based metakaolin geopolymers up to 1200 °C was also examined by Jaya et al. [212] in terms of shrinkage and microstructural changes. The optimum densification temperature increases with the addition of quartz sand or alumina powder. When fly ash and metakaolin geopolymers were compared, it was shown that the latter are more tolerant of high temperatures [213]. To improve the thermal characteristics of geopolymer, fibers such as ash wollastonite and basalt fibers could be incorporated. Furthermore, porous materials could serve as a thermal barrier. One of the most important research areas is the creation of lightweight porous materials. Faster construction, improved thermal performance, and fire resistance are all advantages of lightweight building materials. During the foaming process, small pores or linked voids can be added to lightweight porous geopolymer materials which are also known as geopolymer foams. Air bubbles or endogenous gas production could be used to introduce the foam like hydrogen peroxide, aluminum powder or sodium hypochlorite. The gas-forming ingredient in this experiment was hydrogen peroxide. Equation (12) illustrates how hydrogen peroxide breaks down into water and oxygen in an alkaline atmosphere.

$$H_2O_2 \rightarrow 2H_2O + O_2 \quad (12)$$

Regarding the foamed geopolymers' thermal characteristics Cheng-Yong et al. [213], found that when the lightweight porous geopolymer based on glass cullet and red mud were subjected to temperatures between 600 and 800 °C, their volume increased. The foamed geopolymer has a strength of more than 2 MPa and a density of less than 866 kg/m$^3$. To create greater strength foamed fly ash geopolymers of between 2 MPa to 30 MPa and with densities less than 1000 kg/m$^3$. Wang et al. [214], utilized 30 percentage slag replacements. The fly ash geopolymer foam maintained its strength well up to 400 °C, and it strengthened much more at 800 °C. According to Cheng-Yong et al. [213], the geopolymer foam did not break or crumble below 1000 °C. Significant shrinkage and sintering are associated with high thermal resistance at high temperatures. As far as we are aware, there is not a lot of literature on the thermal performance and fire resistance of foamed geopolymer materials. Most people believe that porous geopolymer foam behaves similarly to dense geopolymer foam when exposed to high temperatures and fire.

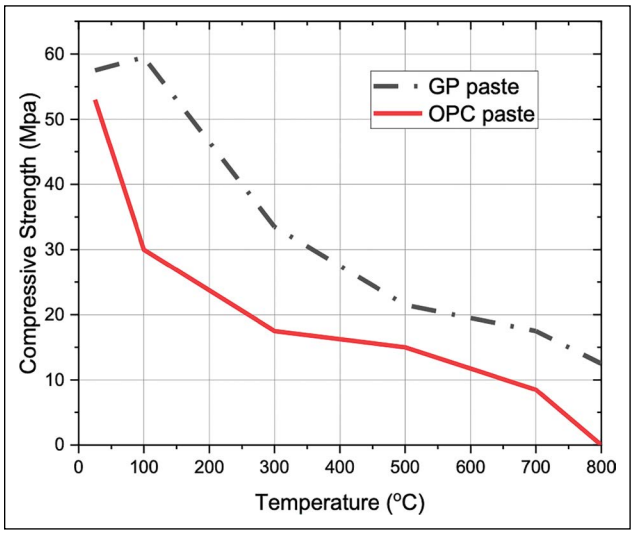


**Figure 6**. Geopolymer and OPC paste compressive strength comparison [215].

In their research on the creation of MK-FA-based geopolymers for applications requiring fire resistance, geopolymers' compressive strength was higher than OPC pastes', according to research by Zhang et al. [215]. As demonstrated in Figure 6, after exposure to 800 °C, geopolymer paste retained 22% of its compressive strength while OPC paste lost all of it.

According to this, MK-FA-based geopolymer paste showed greater compressive strength than OPC paste at room temperature or after being exposed to high temperatures [168]. At temperatures above 400°, the compressive strength of geopolymer concrete typically remains constant and degrades at a rather gradual rate [216]. Work on FA-slag GPL that was heated up to 1000 o C was done by Chithambaram et al. [217]. The weight reduction rate increased as the temperature rose from 200 °C to 1000 °C, regardless of the alkali content. The reduction of the crystalline nature caused by the inclusion of GGBS resulted in increased strength and polymerization. The rate of polymerization slows down as the temperature is raised above 600 °C, which results in a minor loss of strength.

## 5. CONCLUSION

This study demonstrated that natural pozzolans, industrial-by products and agro-wastes are a key precursor in the production of geopolymers. The following conclusions are based on the review articles;

1. The geopolymer mortar/ concrete exhibits high resistance to both chemical and acid attack compared to conventional cements
2. OPC concrete possess a greater carbonation resistance than GPC because of its better binding ability associated with high content of portlandite
3. Increasing the alkali activator concentration to some extend demostrates an increase in resilience to both acid and salts attack
4. Temperature, relative humidity and the period of contact with water contribute to the carbonation mechanism and kinetics
5. Geopolymers has shown excellent resistance to temperature extreme compared to convectional cement.

## 6. AREAS OF FUTURE RESEARCH

There hasn't been any research done on the creation of geopolymer binders using a binary of coconut shell ash and waste from calcined clay bricks. Therefore, based on the research reviewed here, the following topics have been identified for further study in order to decrease the consumption of natural resources and to minimise other environmental effects related to the manufacturing of OPC:

1. Mechanical and durability features of geopolymer cement using alkali-activated calcined clay brick waste from production as well as building sites to ascertain its potential as a geopolymer cement. High alkalinity boasts a higher degree of reaction and maintains a matrix density that tends to prohibit the permeation of corrosive elements into the internal framework of geopolymer cements.
2. Mechanical and durability features of geopolymer cement using alkali-activated coconut shell ash as the primary source materials to ascertain its potential as a geopolymer cement.
3. A blend of alkali-activated coconut shell ash-calcined clay bricks waste mechanical and durability properties to evaluate its binding suitability.
4. Life cycle assessment of geopolymers resulting from coconut shell ash - calcined clay bricks waste to present the sustainability of these products and the potential benefit of such technology.

## ETHICS

There are no ethical issues with the publication of this manuscript.

## DATA AVAILABILITY STATEMENT

The authors confirm that the data that supports the findings of this study are available within the article. Raw data that support the finding of this study are available from the corresponding author, upon reasonable request.

## CONFLICT OF INTEREST

The authors declare that they have no conflict of interest.

## FINANCIAL DISCLOSURE

The authors declared that this study has received no financial support.

## PEER-REVIEW

Externally peer-reviewed.

## REFERENCES

[1] Datau, S. G., Bawa, M. A., Jatau, J. S., Muhammad, M. H., & Bello, A. S. (2020). The potentials of kyanite particles and coconut shell ash as strengthener in aluminum alloy composite for automobile brake disc. *Journal of Minerals and Materials Characterization and Engineering*, 8(3), 84–96. [CrossRef]

[2] Minkova, V., Marinov, S. P., Zanzi, R., Björnbom, E., Budinova, T., Stefanova, M., & Lakov, L. (2000). Thermochemical Treatment of Biomass in a Flow of Steam or in a Mixture of Steam and Carbon Dioxide. *Fuel Processing Technology*, 62(1), 45–52. [CrossRef]

[3] Putun, A. E., Ozbay, N., Onal, E. P., & Putun, E. (2005). Fixed-bed pyrolysis of cotton stalk for liquid and solid products. *Fuel Processing Technology*, 86(11), 1207–1219. [CrossRef]

[4] Savova, D., Apak, E., Ekinci, E., Yardim, F., Petrov, N., Budinova, T., Razvigorova, M., & Minkova, V. (2001). Biomass conversion to carbon adsorbents and gas. *Biomass and Bioenergy*, 21(2), 133–142. [CrossRef]

[5] Tsai, W., Chang, C. Y., & Lee, S. L. (1997). Preparation and characterization of activated carbons from corn cob. *Carbon*, 35(8), 1198–1200. [CrossRef]

[6] Intiya, W., Thepsuwan, U., Sirisinha, C., & Sae-Oui, P. (2017). Possible use of sludge ash as filler in natural rubber. *Journal of Material Cycles and Waste Management*, 19(2), 774–781. [CrossRef]

[7] Jalali, M., & Aboulghazi, F. (2013). Sunflower stalk, an agricultural waste, as an adsorbent for the removal of lead and cadmium from aqueous solutions. *Journal of Material Cycles and Waste Management*, 15(4), 548–555. [CrossRef]

[8] Fan, M., Marshall, W., Daugaard, D., & Brown, R. C. (2004). Steam activation of chars produced from oat hulls and corn stover. *Bioresource Technology*, 93(1), 103–107. [CrossRef]

[9] Ahmedna, M., Marshall, W. E., & Rao, R. M. (2000). Production of granular activated carbons from select agricultural by-products and evaluation of their physical, chemical and adsorption properties. *Bioresource Technology*, 71(2), 113–123. [CrossRef]

[10] El-Dakroury, A., & Gasser, M. S. (2008). Alkali-activated materials. *Journal of Nuclear Materials*, 381(3), 271–277. [CrossRef]

[11] Asavapisit, S., & Macphee, D. E. (2007). Immobilization of metal-containing waste in alkali-activated lime–RHA cementitious matrices. *Cement and Concrete Research*, 37(5), 776–780. [CrossRef]

[12] Nair, D. G., Jagadish, K. S., & Fraaij, A. (2006). Reactive pozzolanas from rice husk ash: An alternative to cement for rural housing. *Cement and Concrete Research*, 36(6), 1062–1071. [CrossRef]

[13] Salas, D. A., Ramirez, A. D., Ulloa, N., Baykara, H., & Boero, A. J. (2018). Life cycle assessment of geopolymer concrete. *Construction and Building Materials*, 190, 170–177. [CrossRef]

[14] Elbasir O. (2020). Influence of cement content on the compressive strength and engineering properties of palm oil fuel ash-based hybrid alkaline cement. Influence of cement content on the compressive strength and engineering properties of palm oil fuel ash-based hybrid alkaline cement. *Third International Conference on Technical Sciences* (ICST2020), 28 - 30 November 2020, Tripoli – Libya.

[15] Kim, D., Lai, H. T., Chilingar, G. V., & Yen, T. F. (2006). Geopolymer formation and its unique properties. *Environmental Geology*, 51(1), 103–111. [CrossRef]

[16] Zhang, Y. J., Wang, Y. C., Xu, D. L., Li, S. (2010). Mechanical performance and hydration mechanism of geopolymer composite reinforced by resin. *Materials Science and Engineering*, 527(24-25), 6574–6580. [CrossRef]

[17] Juenger, M. C. G., Winnefeld, F., Provis, J. L., Ideker, J. H. (2011). Advances in alternative cementitious binders. *Cement and Concrete Research*, 41(12), 1232–1243. [CrossRef]

[18] Duxson, P., Provis, J. L., Lukey, G. C., & Van Deventer, J. S. (2007). The role of inorganic polymer technology in the development of 'Green Concrete'. *Cement And Concrete Research*, 37(12), 1590–1597. [CrossRef]

[19] Duxson, P., Fernández-Jiménez, A., Provis, J. L., Lukey, G. C., Palomo, A., & Van Deventer, J. S. (2007). Geopolymer technology: The current state of the art. *Journal of Materials Science*, 42(9), 2917–2933. [CrossRef]

[20] Palomo, A., Grutzeck, M. W., & Blanco, M. T. (1999). Alkali-activated fly ashes: A cement for the future. *Cement and Concrete Research*, 29(8), 1323–1329. [CrossRef]

[21] Behera, M., Bhattacharyya, S. K., Minocha, A. K., Deoliya, R., & Maiti, S. (2014). Recycled aggregate from C&D waste & its use in concrete–A breakthrough towards sustainability in construction sector: A review. *Construction and Building Materials*, 68, 501–516. [CrossRef]

[22] McLellan, B. C., Williams, R. P., Lay, J., Van Riessen, A., & Corder, G. D. (2011). Costs and carbon emissions for geopolymer pastes in comparison to ordinary Portland cement. *Journal of Cleaner Production*, 19(9-10), 1080–1090. [CrossRef]

[23] Xu, H.P., & Deventer, J.V. (2003). Effect of source materials on geopolymerization. *Industrial & Engineering Chemistry Research*, 42(8), 1698–1706. [CrossRef]

[24] Akcaoglu, T., Cubukcuoglu, B., & Awad, A. (2019). A critical review of slag and fly-ash based geopolymer concrete. *Computers and Concrete*, 24(5), 453–458.

[25] Wang, W., Liu, X., Guo, L., & Duan, P. (2019). Evaluation of properties and microstructure of cement paste blended with metakaolin subjected to high temperatures. *Materials*, 12(6), Article 941. [CrossRef]

[26] Wang, K. (2004). *Proceedings of the International Workshop on Sustainable Development and Concrete Technology*, Beijing, China, May 20-21, 2004. Center for Transportation Research and Education, Iowa State University; 2004.

[27] Khale, D., & Chaudhary, R. (2007). Mechanism of geopolymerization and factors influencing its development: A review. *Journal of Materials Science*, 42(3), 729–746. [CrossRef]

[28] Oh, J. E., Monteiro, P. J., Jun, S. S., Choi, S., & Clark, S. M. (2010). The evolution of strength and crystalline phases for alkali-activated ground blast furnace slag and fly ash-based geopolymers. *Cement and Concrete Research*, 40(2), 189–196. [CrossRef]

[29] Garcia-Lodeiro, I., Donatello, S., Fernández-Jimenez, A., & Palomo, A. (2013). Basic principles of hybrid alkaline cements. *Romanian Journal of Materials*, 42(4), 330–335.

[30] Palomo, Á., Maltseva, O., García-Lodeiro, I., & Fernández-Jiménez, A. (2013). Hybrid alkaline cements. Part II: The clinker factor. *Romanian Journal of Materials*, 43(1), 74–80.

[31] Garcia-Lodeiro, I., Fernandez-Jimenez, A., & Palomo, A. (2013). Hydration kinetics in hybrid binders: Early reaction stages. *Cement and Concrete Composites*, 39, 82–92. [CrossRef]

[32] Provis, J. L. (2018). Alkali-activated materials. *Cement and Concrete Research*, 114, 40–48. [CrossRef]

[33] Singh, B., Ishwarya, G., Gupta, M., & Bhattacharyya, S. K. (2015). Geopolymer concrete: A review of some recent developments. *Construction and Building Materials*, 85, 78–90. [CrossRef]

[34] Naveena, K., & Rao, H. S. (2016). A review on strength and durability studies on geopolymer concrete produced with recycled aggregates. *International Journal for Scientific Research and Development*, 4(07), 27–30.

[35] Givi, A. N., Rashid, S. A., Aziz, F. N. A., & Salleh, M. A. M. (2010). Contribution of rice husk ash to the properties of mortar and concrete: A review. *Journal of American Science*, 6(3), 157–165.

[36] Feng, D., Provis, J. L., & Van Deventer, J. S. J. (2012). Thermal activation of albite for the synthesis of one-part mix geopolymers. *Journal of the American Ceramic Society*, 95(2), 565–572. [CrossRef]

[37] Duxson, P., & Provis, J. L. (2008). Designing precursors for geopolymer cements. *Journal of The American Ceramic Society*, 91(12), 3864–3869. [CrossRef]

[38] Koloušek, D., Brus, J., Urbanova, M., Andertova, J., Hulinsky, V., & Vorel, J. (2007). Preparation, structure and hydrothermal stability of alternative (sodium silicate-free) geopolymers. *Journal of Materials Science*, 42(22), 9267–9275. [CrossRef]

[39] Samadhi, T. W., Wulandari, W., Prasetyo, M.I., & Fernando MR. (2017). Reuse of coconut shell, rice husk, and coal ash blends in geopolymer synthesis. IOP Conference Series: *Materials Science and Engineering*, 248, Article 012008. [CrossRef]

[40] Xu, H., & Van Deventer, J. S. J. (2000). The geopolymerisation of alumino-silicate minerals. *International Journal of Mineral Processing*, 59(3), 247–266. [CrossRef]

[41] Provis, J. L., Palomo, A., & Shi, C. (2015). Advances in understanding alkali-activated materials. *Cement and Concrete Research*, 78, 110–125. [CrossRef]

[42] Mucsi, G., & Ambrus, M. (2017). Raw materials for geopolymerisation. In: *The Publications of the MultiScience - XXXI. MicroCAD International Scientific Conference*. University of Miskolc, 2017. [CrossRef]

[43] Mucsi, G., Kumar, S., Csőke, B., Kumar, R., Molnár, Z., Rácz, Á., Mádai, F., & Debreczeni, Á. (2015). Control of geopolymer properties by grinding of land filled fly ash. *International Journal of Mineral Processing*, 143, 50–58. [CrossRef]

[44] Balczár, I., Korim, T., Kovács, A., & Makó, É. (2016). Mechanochemical and thermal activation of kaolin for manufacturing geopolymer mortars–comparative study. *Ceramics International*, 42(14), 15367–15375. [CrossRef]

[45] Rashad, A. M. (2013). Metakaolin as cementitious material: History, scours, production and composition–A comprehensive overview. *Construction and Building Materials*, 41, 303–318. [CrossRef]

[46] Tironi, A., Trezza, M. A., Scian, A. N., & Irassar, E. F. (2013). Assessment of pozzolanic activity of different calcined clays. *Cement and Concrete Composites*, 37, 319–327. [CrossRef]

[47] Vizcayno, C., De Gutierrez, R. M., Castelló, R., Rodríguez, E., & Guerrero, C. E. (2010). Pozzolan obtained by mechanochemical and thermal treatments of kaolin. *Applied Clay Science*, 49(4), 405–413. [CrossRef]

[48] Marangu, J. M., Riding, K., Alaibani, A., Zayed, A., Thiong'o, J. K., & Wachira, J. M. (2020). Potential for selected kenyan clay in production of limestone calcined clay cement. Springer. [CrossRef]

[49] Yip, C. K., & Van Deventer, J. S. J. (2003). Microanalysis of calcium silicate hydrate gel formed within a geopolymeric binder. *Journal of Materials Science*, 38(18), 3851–3860. [CrossRef]

[50] Charles, E. W., & Lin DP. (2009). The chemistry of clay minerals weaver. Charles E.; Pollard, Lin D. 2009. https://masterpdf.pro/download/4330427-the-chemistry-of-clay-minerals-weaver-charles-e-pollard-lin-d Accessed September 9, 2022.

[51] Kadhim, A., Sadique, M., Al-Mufti, R., & Hashim, K. (2021). Developing one-part alkali-activated metakaolin/natural pozzolan binders using lime waste. *Advances in Cement Research*, 33(8), 342–356. [CrossRef]

[52] Rocha, J., & Klinowski, J. (1990). Solid-state NMR studies of the structure and reactivity of metakaolinite. *Angewandte Chemie International Edition*, 29(5), 553–554. [CrossRef]

[53] Mlinárik, L., & Kopecskó, K. (2013). Impact of metakaolin - a new supplementary material - on the hydration mechanism of cements. *Civil Engineering*, 56(2), Article 11.

[54] Ngui, F. M., Wachira, J. M., Thiong'o, J. K., & Marangu, J. M. (2019). Performance of Ground Clay Brick Mortars in Simulated Chloride and Sulphate Media. *Journal of Engineering*, 2019, Article 6430868. [CrossRef]

[55] Dubois, J., Murat, M., Amroune, A., Carbonneau, X., & Gardon, R. (1995). High-temperature transformation in Kaolinite: The role of the crystallinity and of the firing atmosphere. *Applied Clay Science*, 10(3), 187–198. [CrossRef]

[56] Shvarzman, A., Kovler, K., Grader, G. S., & Shter, G. E. (2003). The effect of dehydroxylation/amorphization degree on pozzolanic activity of kaolinite. *Cement and Concrete Research*, 33(3), 405–416. [CrossRef]

[57] Sha, W., & Pereira, G. B. (2001). Differential scanning calorimetry study of ordinary Portland cement paste containing metakaolin and theoretical approach of metakaolin activity. *Cement and Concrete Composites*, 23(6), 455–461. [CrossRef]

[58] Zhang, Z., Provis, J. L., Reid, A., & Wang, H. (2014). Geopolymer foam concrete: An emerging material for sustainable construction. *Construction and Building Materials*, 56, 113–127. [CrossRef]

[59] Provis, J. L., & Bernal, S. A. (2014). Geopolymers and related alkali-activated materials. *Annual Review of Materials Research*, 44, 299–327. [CrossRef]

[60] Toniolo, N., & Boccaccini, A. R. (2017). Fly ash-based geopolymers containing added silicate waste. A review. *Ceramics International*, 43(17), 14545–14551. [CrossRef]

[61] Payá, J., Monzó, J., Borrachero, M. V., & Tashima, M. M. (2015). Reuse of Aluminosilicate Industrial Waste Materials in the Production of Alkali-Activated Concrete Binders. *In Handbook of Alkali-Activated Cements, Mortars and Concretes*. F. Pacheco-Torgal, J. A. Labrincha, C. Leonelli, A. Palomo, P. Chindaprasirt, (Eds.), (pp. 487–518). Woodhead Publishing. [CrossRef]

[62] Arafa, S. A., Ali, A. Z. M., Awal, A. S. M. A., & Loon, L. Y. (2018). Optimum mix for fly ash geopolymer binder based on workability and compressive strength. *IOP Conference Series: Earth and Environmental Science*, 140, Article 012157. [CrossRef]

[63] Komnitsas, K., & Zaharaki, D. (2007). Geopolymerisation: A review and prospects for the minerals industry. *Minerals Engineering*, 20(14), 1261–1277. [CrossRef]

[64] Swanepoel, J. C., & Strydom, C. A. (2002). Utilisation of fly ash in a geopolymeric material. *Applied Geochemistry,* 17(8), 1143–1148. [CrossRef]

[65] Kumar, S., Djobo, J. N. Y., Kumar, A., & Kumar, S. (2016). Geopolymerization behavior of fine iron-rich fraction of brown fly ash. *Journal of Building Engineering*, 8, 172–178. [CrossRef]

[66] Lloyd, R. R., Provis, J. L., & Van Deventer, J. S. (2009). Microscopy and microanalysis of inorganic polymer cements. 2: The gel binder. *Journal of Materials Science*, 44(2), 620–631. [CrossRef]

[67] Kumar, S., Kumar, R., & Mehrotra, S. P. (2010). Influence of granulated blast furnace slag on the reaction, structure and properties of fly ash based geopolymer. *Journal of Materials Science*, 45(3), 607–615. [CrossRef]

[68] Higuera, I., Varga, C., Palomo, J. G., Gil-Maroto, A., Vázquez, T., Puertas, F. (2012). Mechanical behaviour of alkali-activated blast furnace slag-activated me-takaolin blended pastes, Statistical study. *Materiales de Construcción*, 62(306):163–181. [CrossRef]

[69] Roy, D. M. (1999). Alkali-activated cements opportunities and challenges. *Cement and Concrete Research*, 29(2), 249–254. [CrossRef]

[70] Yip, C. K., Lukey, G. C., & van Deventer Dean, J. S. J. (2012). Effect of blast furnace slag addition on microstructure and properties of metakaolinite geopolymeric materials. In: N. P. Bansal, J. P. Singh, W.M. Kriven, H. Schneider, (Eds,). *Ceramic Transactions Series* (pp. 187–209). John Wiley & Sons, Inc. [CrossRef]

[71] Buchwald, A., Hilbig, H., & Kaps, C. (2007). Alkali-activated metakaolin-slag blends—performance and structure in dependence of their composition. *Journal of Materials Science*, 42(9), 3024–3032. [CrossRef]

[72] Hadi, M. N., Farhan, N. A., & Sheikh, M. N. (2017). Design of geopolymer concrete with GGBFS at ambient curing condition using Taguchi method. *Construction and Building Materials*, 140, 424–431. [CrossRef]

[73] Hasnaoui, A., Ghorbel, E., & Wardeh, G. (2021). Effect of curing conditions on the performance of geopolymer concrete based on granulated blast furnace slag and metakaolin. *Journal of Materials in Civil Engineering*, 33(3), Article 04020501. [CrossRef]

[74] Dani, M., Borad, J., & Shukla, R. (2015). Review on utilization ofmodified red mud by organic modifier in composite material. *International Journal of Advance Research in Science and Engineering*, 4(3), 216–225. [CrossRef]

[75] Alshaaer, M., & Jeon, H. Y. (2020). *Geopolymers and other geosynthetics*. Intech Open. [CrossRef]

[76] Kumar, A., & Kumar, S. (2013). Development of paving blocks from synergistic use of red mud and fly ash using geopolymerization. *Construction and Building Materials*, 38, 865–871. [CrossRef]

[77] Liang, X., & Ji, Y. (2021). Experimental study on durability of red mud-blast furnace slag geopolymer mortar. *Construction and Building Materials*, 267, Article 120942. [CrossRef]

[78] Mucsi G., Szabó, R., Rácz, Á., Kristály, F., & Kumar S. (2019). Combined utilization of red mud and mech,anically activated fly ash in geopolymer. *Rudarsko-Geološko-Naftni Zbornik*. 34(1), Article 44. [CrossRef]

[79] Vance, E. R., Perera, R., Imperia, D. S., Cassidy, P., Davis, D. J., & Gourley, J. T. (2009). Perlite waste as a precursor for geopolymer formation. *Journal of the Australian Ceramic Society*, 45(1), 44-49. [CrossRef]

[80] Vaou, V., & Panias, D. (2010). Thermal insulating foamy geopolymers from perlite. *Minerals Engineering*, 23(14), 1146–1151. [CrossRef]

[81] Fernández-Jiménez, A., García-Lodeiro, I., & Palomo, A. (2007). Durability of alkali-activated fly ash cementitious materials. *Journal of Materials Science*, 42(9), 3055–3065. [CrossRef]

[82] Shi, C., Jiménez, A. F., & Palomo, A. (2011). New cements for the 21st century: The pursuit of an alternative to Portland cement. *Cement and Concrete Research*, 41(7), 750–763. [CrossRef]

[83] Davidovits, J. (1991). Geopolymers: Inorganic polymeric new materials. *Journal of Thermal Analysis and Calorimetry*, 37(8), 1633–1656. [CrossRef]

[84] Catauro, M., Dal Poggetto, G., Sgarlata, C., Ciprioti, S. V., Pacifico, S., & Leonelli, C. (2020). Thermal and microbiological performance of metakaolin-based geopolymers cement with waste glass. *Applied Clay Science*, 197, Article 105763. [CrossRef]

[85] Yousef, R. I., El-Eswed, B., Alshaaer, M., Khalili, F., & Rahier, H. (2012). Degree of reactivity of two kaolinitic minerals in alkali solution using zeolitic tuff or silica sand filler. *Ceramics International*, 38(6), 5061–5067.

[86] Davidovits J. (1994). Properties of geopolymer cements. Geopolymer Institue. [CrossRef]

[87] Khan, H. A., Castel, A., & Khan, M. S. (2020). Corrosion investigation of fly ash based geopolymer mortar in natural sewer environment and sulphuric acid solution. *Corrosion Science*, 168, Article 108586. [CrossRef]

[88] Yan, B., Duan, P., & Ren, D. (2017). Mechanical strength, surface abrasion resistance and microstructure of fly ash-metakaolin-sepiolite geopolymer composites. *Ceramics International*, 43(1), 1052–1060.

[89] Shima, P., Szczotok, A. M., Rodríguez, J. F., Valentini, L., & Lanzón, M. (2016). Effect of freeze-thaw cycles on the mechanical behavior of geopolymer concrete and Portland cement concrete containing micro-encapsulated phase change materials. Elsevier Enhanced Reader. [CrossRef]

[90] Zhao, R., Yuan, Y., Cheng, Z., Wen, T., Li, J., Li, F., & Ma, Z. J. (2019). Freeze-thaw resistance of Class F fly ash-based geopolymer concrete. *Construction and Building Materials*, 222, 474–483. [CrossRef]

[91] Huseien, G. F., & Shah, K. W. (2020). Durability and life cycle evaluation of self-compacting concrete containing fly ash as GBFS replacement with alkali activation. *Construction and Building Materials*, 235, Article 117458. [CrossRef]

[92] Puertas, F., & Fernández-Jiménez, A. (2003). Mineralogical and microstructural characterisation of alkali-activated fly ash/slag pastes. *Cement and Concrete Composites*, 25(3), 287–292. [CrossRef]

[93] Detwiler R. J., & Taylor P. C. (2005). Specifier's guide to durable concrete. Engineering Bulletin 221, https://trid.trb.org/view/900218 Accessed on Sep 27, 2022.

[94] Faten, S., Hani, K., Hubert, R., & Jan, W. (2015). Durability of alkali activated cement produced from kaolinitic clay. *Applied Clay Science*, 104, 229–237. [CrossRef]

[95] Chen, K., Wu, D., Xia, L., Cai, Q., Zhang, Z. (2021). Geopolymer concrete durability subjected to aggressive environments – A review of influence factors and comparison with ordinary Portland cement. *Construction and Building Materials*, 279, Article 122496. [CrossRef]

[96] Koenig, A., & Dehn, F. (2016). Main considerations for the determination and evaluation of the acid resistance of cementitious materials. *Materials and Structures*, 49(5), 1693–1703. [CrossRef]

[97] Temuujin, J., Minjigmaa, A., Lee, M., Chen-Tan, N., & Van Riessen, A. (2011). Characterisation of class F fly ash geopolymer pastes immersed in acid and alkaline solutions. *Cement and Concrete Composites*, 33(10), 1086–1091. [CrossRef]

[98] Matalkah, F., Soroushian, P., Balchandra, A., & Peyvandi, A. (2017). Characterization of Alkali-Activated Nonwood Biomass Ash–Based Geopolymer Concrete. *Journal of Materials in Civil Engineering*, 29(4), Article 04016270. [CrossRef]

[99] Bakharev, T. (2005). Resistance of geopolymer materials to acid attack. *Cement and Concrete Research*, 35(4), 658–670. [CrossRef]

[100] Bouguermouh, K., Bouzidi, N., Mahtout, L., Pérez-Villarejo, L., Lourdes, M., & Martínez-Cartas, M. L. (2017). Effect of acid attack on microstructure and composition of metakaolin-based geopolymers: The role of alkaline activator. *Journal of Non-Crystalline Solids*, 463, 128–137. [CrossRef]

[101] Ariffin, M. A. M., Bhutta, M. A. R., Hussin, M. W., Tahir, M. M., & Aziah, N. (2013). Sulfuric acid resistance of blended ash geopolymer concrete. *Construction and Building Materials*, 43, 80–86. [CrossRef]

[102] Sata, V., Sathonsaowaphak, A., & Chindaprasirt, P. (2012). Resistance of lignite bottom ash geopolymer mortar to sulfate and sulfuric acid attack. *Cement and Concrete Composites*, 34(5), 700–708. [CrossRef]

[103] Bernal, S. A., Rodríguez, E. D., Mejía de Gutiérrez, R., & Provis, J. L. (2012). Performance of alkali-activated slag mortars exposed to acids. *Journal of Sustainable Cement-Based Materials*, 1(3), 138–151. [CrossRef]

[104] Dimas, D., Giannopoulou, I., & Panias, D. (2009). Polymerization in sodium silicate solutions: a fundamental process in geopolymerization technology. *Journal of Materials Science*, 44(14), 3719–3730. [CrossRef]

[105] Ajay, A., Ramaswamy, K. P., & Thomas, A. V. (2020). A critical review on the durability of geopolymer composites in acidic environment. *IOP Conference Series: Earth and Environmental Science*, 491(1), Article 012044. [CrossRef]

[106] Chen-Tan, N. W., Van Riessen, A., Ly, C. V., & Southam, D. C. (2009). Determining the] reactivity of a fly ash for production of geopolymer. *Journal of the American Ceramic Society*, 92(4), 881–887. [CrossRef]

[107] Koenig, A., Herrmann, A., Overmann, S., & Dehn, F. (2017). Resistance of alkali-activated binders to organic acid attack: Assessment of evaluation criteria and damage mechanisms. *Construction and Building Materials*, 151, 405–413. [CrossRef]

[108] Roy, D. M., Arjunan, P., & Silsbee, M. R. (2001). Effect of silica fume, metakaolin, and low-calcium fly ash on chemical resistance of concrete. *Cement and Concrete Research*, 31(12), 1809–1813.

[109] Shi, C., & Stegemann, J. A. (2000). Acid corrosion resistance of different cementing materials. *Cement and Concrete Research*, 30(5), 803–808. [CrossRef]

[110] Mori, T., Nonaka, T., Tazaki, K., Koga, M., Hikosaka, Y., & Noda, S. (1992). Interactions of nutrients, moisture and PH on microbial corrosion of concrete sewer pipes. *Water Research*, 26(1), 29–37. [CrossRef]

[111] Davis, J. L., Nica, D., Shields, K., & Roberts, D. J. (1998). Analysis of concrete from corroded sewer pipe. *International Biodeterioration & Biodegradation*, 42(1), 75–84. [CrossRef]

[112] Marquez-Peñaranda, J. F., Sanchez-Silva, M., Husserl, J., & Bastidas-Arteaga, E. (2016). Effects of biodeterioration on the mechanical properties of concrete. *Materials and Structures*, 49(10), 4085–4099. [CrossRef]

[113] Pacheco-Torgal, F., Castro-Gomes, J., & Jalali, S. (2008). Alkali-activated binders: A review: Part 1. Historical background, terminology, reaction mechanisms and hydration products. *Construction and Building Materials*, 22(7), 1305–1314. [CrossRef]

[114] Bernal, S. A., Provis, J. L., Rose, V., & De Gutiérrez, R. M. (2013). High-resolution X-ray diffraction and fluorescence microscopy characterization of alkali-activated slag-metakaolin binders. *Journal of The American Ceramic Society*, 96(6), 1951–1957. [CrossRef]

[115] Davidovits, J. (1994). Geopolymers: man-made rock geosynthesis and the resulting development of very early high strength cement. *Journal of Materials Education*, 16(2-3), 91–139.

[116] Lee, N. K., & Lee, H. K. (2016). Influence of the slag content on the chloride and sulfuric acid resistances of alkali-activated fly ash/slag paste. *Cement and Concrete Composites*, 72, 168–179. [CrossRef]

[117] Bondar, D., Lynsdale, C. J., Milestone, N. B., & Hassani, N. (2015). Sulfate resistance of alkali activated pozzolans. *International Journal of Concrete Structures and Materials*, 9(2), 145–158. [CrossRef]

[118] Lloyd, R. R., Provis, J. L., & Van Deventer, J. S. (2012). Acid resistance of inorganic polymer binders. 1. Corrosion rate. *Materials and Structures*, 45(1), 1–14. [CrossRef]

[119] Bakharev T. (2005). Geopolymeric materials prepared using Class F fly ash and elevated temperature curing. *Cement and Concrete Research*, 35(6), 1224–1232. [CrossRef]

[120] Senhadji, Y., Escadeillas, G., Mouli, M., Benosman, A. S., & Khelafi, H. (2014). Influence of natural pozzolan, silica fume and limestone fine on strength, acid resistance and microstructure of mortar. *Powder Technology*, 254, 314–323. [CrossRef]

[121] Thokchom, S., Dutta, D., & Ghosh, S. (2011). Effect of incorporating silica fume in fly ash geopolymers. *International Journal of Civil and Environmental Engineering*, 5(12), 750–754.

[122] Purbasari, A., Samadhi, T. W., & Bindar, Y. (2012). Sulfuric acid resistance of geopolymer mortars from co-combustion residuals of bamboo and kaolin. *ASEAN Journal of Chemical Engineering*, 18(2), 22–30.

[123] Lavanya, G., & Jegan, J. (2015). Durability study on high calcium fly ash based geopolymer concrete. Advances in *Materials Science and Engineering*, 6, 1–7. [CrossRef]

[124] Song, Y., Liu, J., Hui, Wang., & Shu, H. (2019). Research progress of nitrite corrosion inhibitor in concrete. *International Journal of Corrosion*, 5, 1–9. [CrossRef]

[125] Kumaravel, S., & Girija, K. (2013). Acid and salt resistance of geopolymer concrete with varying concentration of NaOH. *Journal of Engineering Research and Studies*, 4(4), 1–3.

[126] Ramaswamy, K. P., & Santhanam, M. (2019). Degradation kinetics of cement-based materials in citric acid. In A. R. M. Rao, & K. Ramanjaneyulu (Eds.), *Recent Advances in Structural Engineering, Volume 1* (pp. 891–905). Springer. [CrossRef]

[127] Suiryanrayna, M. V., & Ramana, J. V. (2015). A review of the effects of dietary organic acids fed to swine. *Journal of Animal Science and Biotechnology*, 6(1), 1–11. [CrossRef]

[128] Ukrainczyk, N., Muthu, M., Vogt, O., & Koenders, E. (2019). Geopolymer, calcium aluminate, and Portland cement-based mortars: Comparing degradation using acetic acid. *Materials*, 12(19), Article 3115. [CrossRef]

[129] Xie, F., Li, J., Zhao, G., Zhou, P., & Zheng, H. (2020). Experimental study on performance of cast-in-situ recycled aggregate concrete under different sulfate attack exposures. *Construction and Building Materials*, 253, Article 119144. [CrossRef]

[130] Villa, C., Pecina, E. T., Torres, R., & Gómez, L. (2010). Geopolymer synthesis using alkaline activation of natural zeolite. *Construction and Building Materials*, 24(11), 2084–2090. [CrossRef]

[131] Alcamand, H. A., Borges, P. H., Silva, F. A., & Trindade, A. C. C. (2018). The effect of matrix composition and calcium content on the sulfate durability of metakaolin and metakaolin/slag alkali-activated mortars. *Ceramics International*, 44(5), 5037–5044. [CrossRef]

[132] Taylor, H. F. W. (1997). *Cement Chemistry* (2nd ed.). Thomas Telford Publishing. [CrossRef]

[133] Menéndez, E., Matschei, T., & Glasser, F. P. (2013). Sulfate attack of concrete. In: M. Alexander, A. Bertron, N. De Belie, (Eds,). *Performance of Cement-Based Materials in Aggressive Aqueous Environments* (pp. 7–74). Vol 10. RILEM State-of-the-Art Reports. Springer. [CrossRef]

[134] Alexander, M., Bertron, A., & De Belie, N., (Eds.). (2013). *Performance of Cement-Based Materials in Aggressive Aqueous Environments: State-of-the-Art Report*. RILEM TC 211 - PAE. Vol 10. Springer. [CrossRef]

[135] Elyamany, H. E., Abd Elmoaty, M., & Elshaboury, A. M. (2018). Magnesium sulfate resistance of geopolymer mortar. *Construction and Building Materials*, 184, 111–127. [CrossRef]

[136] Ismail, I., Bernal, S. A., Provis, J. L., Hamdan, S., & Van Deventer, J. S. (2013). Microstructural changes in alkali activated fly ash/slag geopolymers with sulfate exposure. *Materials and Structures*, 46(3), 361–373.

[137] Ismail, I., Bernal, S. A., Provis, J. L., San Nicolas, R., Brice, D. G., Kilcullen, A. R., Hamdan, S., & Van Deventer, J. S. (2013). Influence of fly ash on the water and chloride permeability of alkali-activated slag mortars and concretes. *Construction and Building Materials*, 48, 1187–1201. [CrossRef]

[138] Chithambar Ganesh, A., Rajesh Kumar, K., Vinod Kumar, M., et al. (2020). Durability Studies on the Hybrid Fiber reinforced Geopolymer concrete made of M-sand under ambient curing. *IOP Conf Ser: Mater Sci Eng.* 981(3):032074. doi:10.1088/1757-899X/981/3/032074. [CrossRef]

[139] Albitar, M., Ali, M. M., Visintin, P., & Drechsler, M. (2017). Durability evaluation of geopolymer and conventional concretes. *Construction and Building Materials*, 136, 374–385. [CrossRef]

[140] Gupta, A., Gupta, N., Saxena, K. K. (2021). Experimental study of the mechanical and durability properties of Slag and Calcined Clay based geopolymer composite. *Advances in Materials and Processing Technologies*, 10, 1–15.

[141] Thokchom, S., Ghosh, P., & Ghosh, S. (2009). Acid resistance of fly ash based geopolymer mortars. *International Journal of Recent Trends in Engineering*, 1(6), 36-40.

[142] Choi, Y. S., Kim, J. G., & Lee, K. M. (2006). Corrosion behavior of steel bar embedded in fly ash concrete. *Corrosion Science*, 48(7), 1733–1745. [CrossRef]

[143] Noushini, A., Castel, A., Aldred, J., & Rawal, A. (2020). Chloride diffusion resistance and chloride binding capacity of fly ash-based geopolymer concrete. *Cement and Concrete Composites*, 105, Article 103290. [CrossRef]

[144] Wang, A., Zheng, Y., Zhang, Z., Liu, K., Li, Y., Shi, L., & Sun, D. (2020). The durability of alkali-activated materials in comparison with ordinary Portland cements and concretes: A review. *Engineering*, 6(6), 695–706. [CrossRef]

[145] Yuan, Q., Shi, C., De Schutter, G., Audenaert, K., & Deng, D. (2009). Chloride binding of cement-based materials subjected to external chloride environment–a review. *Construction and Building Materials*, 23(1), 1–13. [CrossRef]

[146] Gunasekara, C., Law, D., Bhuiyan, S., Setunge, S., & Ward, L. (2019). Chloride induced corrosion in different fly ash based geopolymer concretes. *Construction and Building Materials*, 200, 502–513. [CrossRef]

[147] de Oliveira, L. B., De Azevedo, A. R., Marvila, M. T., Pereira, E. C., Fediuk, R., & Vieira, C. M. F. (2022). Durability of geopolymers with industrial waste. *Case Studies in Construction Materials*, 16, Article e00839. [CrossRef]

[148] Zhang, J., Shi, C., & Zhang, Z. (2019). Chloride binding of alkali-activated slag/fly ash cements. *Construction and Building Materials*, 226, 21–31. [CrossRef]

[149] Logesh Kumar, M., & Revathi, V. (2021). Durability Performance On Alkali Activated Metakaolin And Bottom Ash Based Geopolymer Concrete. Preprint. https://doi.org/10.21203/rs.3.rs-703480/v1[CrossRef]

[150] Parveen, S., Pham, T. M., Lim, Y. Y., Pradhan S. S., Jatin, & Kumar, J. (2021). Performance of rice husk Ash-Based sustainable geopolymer concrete with Ultra-Fine slag and Corn cob ash. *Construction and Building Materials*, 279, Article 122526. [CrossRef]

[151] Mashaly, A. O., El-Kaliouby, B. A., Shalaby, B. N., El–Gohary, A. M., & Rashwan, M. A. (2016). Effects of marble sludge incorporation on the properties of cement composites and concrete paving blocks. *Journal of Cleaner Production*, 112, 731–741. [CrossRef]

[152] Saranya, P., Nagarajan, P., & Shashikala, A. P. (2021). Performance studies on steel fiber–Reinforced GGBS-dolomite geopolymer concrete. Journal of Materials in *Civil Engineering*, 33(2), Article 04020447. [CrossRef]

[153] Saxena, R., Gupta, T., Sharma, R. K., & Panwar, N. L. (2021). Influence of granite waste on mechanical and durability properties of fly ash-based geopolymer concrete. *Environment, Development and Sustainability*, 23(12), 17810–17834. [CrossRef]

[154] Sravanthi, D., Himath Kumar, Y., Sarath Chandra Kumar, B.. (2020). Comparative study on flow characteristics, strength and durability of GGBS based geopolymer concrete. IOP Conference Series: *Materials Science and Engineering*, 912(6), Article 062032. [CrossRef]

[155] De Ceukelaire, L., & Van Nieuwenburg, D. (1993). Accelerated carbonation of a blast-furnace cement concrete. *Cement and Concrete Research*, 23(2), 442–452. [CrossRef]

[156] Khan, M. S. H., Castel, A., & Noushini, A. (2017). Carbonation of a low-calcium fly ash geopolymer concrete. *Magazine of Concrete Research*, 69(1), 24–34.

[157] Adamczyk, K., Prémont-Schwarz, M., Pines, D., Pines, E., & Nibbering, E. T. J. (2009). Real-time observation of carbonic acid formation in aqueous solution. *Science*, 326(5960), 1690–1694. [CrossRef]

[158] Dubina, E., Korat, L., Black, L., Strupi-Šuput, J., & Plank, J. (2013). Influence of water vapour and carbon di-oxide on free lime during storage at 80°C, studied by Raman spectroscopy. *Spectrochimica Acta Part A: Molecular and Biomolecular Spectroscopy*, 11, 299– 303. [CrossRef]

[159] Fernández-Díaz, L., Fernández-González, Á., & Prieto, M. (2010). The role of sulfate groups in controlling CaCO3 polymorphism. *Geochimica et Cosmochimi-ca Acta*, 74(21), 6064–6076. [CrossRef]

[160] Johannesson, B., & Utgenannt, P. (2001). Microstructural changes caused by carbonation of cement mortar. *Cement and Concrete Research*, 31(6), 925–931. [CrossRef]

[161] Bernal, S. A., de Gutierrez, R. M., Provis, J. L., & Rose, V. (2010). Effect of silicate modulus and metakaolin incorporation on the carbonation of alkali silicate-activated slags. *Cement and Concrete Research*. 40(6), 898–907. [CrossRef]

[162] Liu, J., Yao, S., Ba, M., He, Z., & Li, Y. (2016). Effects of carbonation on micro structures of hardened cement paste. *Journal Wuhan University of Technology, Materials Science Edition*, 31(1), 146–150. [CrossRef]

[163] Zhang, R., & Panesar, D. K. (2020). Carbonated binder systems containing reactive MgO and Portland cement: Strength, chemical composition and pore structure. *Journal of Cleaner Production*, 271, Article 122021. [CrossRef]

[164] von Greve-Dierfeld, S., Lothenbach, B., Vollpracht, A., Wu, B., Huet, B., Andrade C., Medina, C., Thiel, C., Gruyaert, E., Vanoutrive, H., Saez del Bosque, I. F., Ignjatovic, I., Elsen, J., Provis, J. L., Scrivener, K., Thienel K-C., Sideris, K., Zajac, M., Alderete N., Cizer, Ö., Van den Heede, P., Hooton, R.D., Kamali-Bernard, S., Bernal, S. A., Zhao, Z., Shi, Z., & De Belle, N. (2020). Understanding the carbonation of concrete with supplementary cementitious materials: a critical review by RILEM TC 281-CCC. *Materials and Structure*, 53(6), Article 136. [CrossRef]

[165] Leemann A., & Moro, F. (2016). Carbonation of concrete: the role of CO2 concentration, relative humidity and CO2 buffer capacity. *Materials and Structures*, 50(1), Article 30. [CrossRef]

[166] Huseien, G. F., Sam, A. R. M, Shah, K. W., Mirza, J., & Tahir, M. (2019). Evaluation of alkali-activated mortars containing high volume waste ceramic powder and fly ash replacing GBFS. *Construction and Building Materials*, 210, 78–92. [CrossRef]

[167] Morandeau, A. (2014). Investigation of the carbonation mechanism of CH and C-S-H in terms of kinetics, microstructure changes and moisture properties. *Cement and Concrete Research*, 2014, Article 18. [CrossRef]

[168] Aziz, I. H., Al Bakri Abdullah, M. M., Cheng Yong, H., Yun Ming, L., Hussin, K., Azimi, E. A. (2015). A review on mechanical properties of geopolymer composites for high temperature application. *KEM*, 660, 34–38. [CrossRef]

[169] Pasupathy, K., Berndt, M., Sanjayan, J., Rajeev, P., Cheema, D. S. (2018). Durability performance of precast fly ash–based geopolymer concrete under atmospheric exposure conditions. *Journal of Materials in Civil Engineering*, 30(3), Article 04018007. [CrossRef]

[170] Li, Z., & Li, S. (2020). Effects of wetting and drying on alkalinity and strength of fly ash/slag-activated materials. *Construction and Building Materials*, 254, Article 119069. [CrossRef]

[171] Li, N., Farzadnia, N., & Shi, C. (2017). Microstructural changes in alkali-activated slag mortars induced by accelerated carbonation. *Cement and Concrete Research*, 100, 214–226. [CrossRef]

[172] Vu, T. H., Gowripalan, N., De Silva, P., Paradowska, A., Garbe, U., Kidd, P., & Sirivivatnanon, V. (2020). Assessing carbonation in one-part fly ash/slag geopolymer mortar: Change in pore characteristics using the state-of-the-art technique neutron tomography. *Cement and Concrete Composites*, 114, Article 103759. [CrossRef]

[173] Morla, P., Gupta, R., Azarsa, P., & Sharma, A. (2021). Corrosion evaluation of geopolymer concrete made with fly ash and bottom ash. *Sustainability*, 13(1), Article 398. [CrossRef]

[174] Law, D. W., Adam, A. A., Molyneaux, T. K., Patnaikuni, I., & Wardhono, A. (2015). Long term durability properties of class F fly ash geopolymer concrete. *Materials and Structures*, 48(3), 721–731. [CrossRef]

[175] Li, Z., & Li, S. (2018,). Carbonation resistance of fly ash and blast furnace slag based geopolymer concrete. *Construction and Building Materials*, 163, 668–680. [CrossRef]

[176] Bakharev, T., Sanjayan, J. G., Cheng, Y. B. (2001). Resistance of alkali-activated slag concrete to carbonation. *Cement and Concrete Research*, 31(9), 1277–1283. [CrossRef]

[177] Marcos-Meson, V., Fischer, G., Edvardsen, C., Skovhus, T. L., & Michel, A. (2019). Durability of steel fibre reinforced Concrete (SFRC) exposed to acid attack – a literature review. *Construction and Building Materials*, 200, 490–501. [CrossRef]

[178] Park, J. W., Ann, K. Y., & Cho, C. G. (2015). Resistance of alkali-activated slag concrete to chloride-induced corrosion. *Advances in Materials Science and Engineering*, 2015, 1–7. [CrossRef]

[179] Nkwaju, R. Y., Djobo, J. N. Y., Nouping, J. N. F., Huisken, P. W. M., Deutou, J.G. N., & Courard, L. (2019). Iron-rich laterite-bagasse fibers based geopolymer composite: Mechanical, durability and insulating properties. *Applied Clay Science*, 183, Article 105333. [CrossRef]

[180] Huang, G., Ji, Y., Li, J., Hou, Z., & Jin, C. (2018). Use of slaked lime and Portland cement to improve the resistance of MSWI bottom ash-GBFS geopolymer concrete against carbonation. *Construction and Building Materials*, 166, 290–300. [CrossRef]

[181] Pasupathy, K., Berndt, M., Sanjayan, J., Rajeev, P., & Cheema, D. S. (2017). Durability of low calcium fly ash based geopolymer concrete culvert in a saline environment. *Cement and Concrete Research*, 100, 297–310. [CrossRef]

[182] Yahya, Z., Bakri Abdullah, M. M. A., Jing, L. Y., Li, L.Y., & Razak, R. A. (2020). Seawater exposure effect on fly ash based geopolymer concrete with inclusion of steel fiber. IOP Conference Series: *Materials Science and Engineering*, 743(1), Article 012013. [CrossRef]

[183] Xu, T., Huang, J., Castel, A., Zhao, R., & Yang, C. (2018). Influence of steel–concrete bond damage on the dynamic stiffness of cracked reinforced concrete beams. *Advances in Structural Engineering*, 21(13), 1977–1989. [CrossRef]

[184] Liang, G., Liu, T., Li, H., Dong, B., & Shi, T. (2022). A novel synthesis of lightweight and high-strength green geopolymer foamed material by rice husk ash and ground-granulated blast-furnace slag. *Resources, Conservation and Recycling*. 176, Article 105922. [CrossRef]

[185] Liang, M., Chang, Z., Wan, Z., Gan, Y., Schlangen, E., & Šavija, B. (2022). Interpretable Ensemble-Machine-Learning models for predicting creep behavior of concrete. *Cement and Concrete Composites*, 125, Article 104295. [CrossRef]

[186] Rovnaník, P. (2010). Effect of curing temperature on the development of hard structure of metakaolin-based geopolymer. *Construction and Building Materials*, 24(7), 1176–1183. [CrossRef]

[187] Yusuf, M. O., Megat Johari, M. A., Ahmad, Z. A., & Maslehuddin, M. (2014). Shrinkage and strength of alkaline activated ground steel slag/ultrafine palm oil fuel ash pastes and mortars. *Materials & Design*, 63, 710–718. [CrossRef]

[188] Seneviratne, C., Gunasekara, C., Law, D. W., Setunge, S., & Robert, D. (2020). Creep, shrinkage and permeation characteristics of geopolymer aggregate concrete: long-term performance. *Archive of Civil and Mechanical Engineering*, 20(4), Article 140. [CrossRef]

[189] Mechtcherine, V., & Hans-Wolf Reinhardt, W. (2012). *Application of super absorbent polymers (SAP) in concrete construction*. Springer. [CrossRef]

[190] Slowik, V., & Ju, J. W. (2011). Discrete modeling of plastic cement paste subjected to drying. *Cement and Concrete Composites*, 33(9), 925–935. [CrossRef]

[191] Gettu, R., Patel, A., Rathi, V., Prakasan, S., Basavaraj, S., & Maity, S. (2019). Influence of supplementary cementitious materials on the sustainability parameters of cements and concretes in the Indian context. *Materials and Structures*, 52(1), Article 10. [CrossRef]

[192] Neupane, K., & Hadigheh, S. A. (2021). Sodium hydroxide-free geopolymer binder for prestressed concrete applications. *Construction and Building Materials*, 293, Article 123397. [CrossRef]

[193] Hardjito, D., & Rangan, B. V. (2005). Development and properties of low-calcium fly ash-based geopolymer concrete. Research Report GC 1 Faculty of Engineering Curtin University of Technology Perth, Australia.

[194] Mehta, A., Siddique, R., Ozbakkaloglu, T., Uddin Ahmed Shaikh, F., & Belarbi, R. (2020). Fly ash and ground granulated blast furnace slag-based alkali-activated concrete: Mechanical, transport and microstructural properties. *Construction and Building Materials*, 257, Article 119548. [CrossRef]

[195] Duxson, P., Provis, J. L., Lukey, G. C., Mallicoat, S. W., Kriv-en, W. M., & Van Deventer, J. S. (2005). Understanding the relationship between geopolymer composition, microstructure and mechanical properties. *Colloids and Surfaces A: Physicochemical and Engineering Aspects*, 269(1-3), 47–58. [CrossRef]

[196] Amin, N., Alam, S., & Gul, S. (2016). Effect of thermally activated clay on corrosion and chloride resistivity of cement mortar. *Journal of Cleaner Production*, 111, 155–160. [CrossRef]

[197] Saloni, P., & Pham, T. M. (2020). Enhanced properties of high-silica rice husk ash-based geopolymer paste by incorporating basalt fibers. *Construction and Building Materials*, 245, Article 118422. [CrossRef]

[198] Saha, A. K. (2018). Effect of class F fly ash on the durability properties of concrete. *Sustainable Environment Research*, 28(1), 25–31. [CrossRef]

[199] Khan, M. S. H., Castel, A., & Noushini A. (2017). The effect of adding fibers on dry shrinkage of geopolymer concrete. *Civil Engineering Journal*, 7(12), 2099–2108. [CrossRef]

[200] Frayyeh, Q. J., & Kamil, M. H. (2021). The effect of adding fibers on dry shrinkage of geopolymer concrete. *Civil Engineering Journal*, 7(12), 2099–2108. [CrossRef]

[201] Banthia, N., & Gupta, R. (2006). Influence of polypropylene fiber geometry on plastic shrinkage cracking in concrete. *Cement and Concrete Research*, 36(7), 1263–1267. [CrossRef]

[202] Kani, E. N., & Allahverdi, A. (2011). Investigating shrinkage changes of natural pozzolan based geopolymer cementpaste. *Iranian Journal of Materials Science and Engineering*, 8(3), 50–60.

[203] Nazari, A., Bagheri, A., Sanjayan, J., Yadav, P. N. J. A., & Tariq, H. (2019). A comparative study of void distribution pattern on the strength development between opc-based and geopolymer concrete. *Advances in Materials Science and Engineering*, 2019, Article 1412757. [CrossRef]

[204] Negahban, E., Bagheri, A., & Sanjayan, J. (2021). Pore gradation effect on Portland cement and geopolymer concretes. *Cement and Concrete Composites*, 122, Article 104141. [CrossRef]

[205] Amin, M., Elsakhawy, Y., Abu El-hassan, K., A., Abdelsalam, B. A. (2021). Behavior evaluation of sustainable high strength geopolymer concrete based on fly ash, metakaolin, and slag. *Case Studies in Construction Materials*, 16, Article e00976. [CrossRef]

[206] Aydın, S., & Baradan, B. (2007). Effect of pumice and fly ash incorporation on high temperature resistance of cement-based mortars. *Cement and Concrete Research*, 37(6), 988–995. [CrossRef]

[207] Lahoti, M., Tan, K. H., Yang, E. H. (2019). A critical review of geopolymer properties for structural fire-resistance applications. *Construction and Building Materials*, 221, 514–526. [CrossRef]

[208] Lin, W., Zhou, F., Luo, W., & You, L. (2021). Recycling the waste dolomite powder with excellent consolidation properties: Sample synthesis, mechanical evaluation, and consolidation mechanism analysis. *Construction and Building Materials*, 290, Article 123198. [CrossRef]

[209] Jeon, D., Yum, W. S., Song, H., Sim, S., & Oh, J. E. (2018). The temperature-dependent action of sugar in the retardation and strength improvement of Ca(OH)2-Na2CO3-activated fly ash systems through calcium complexation. *Construction and Building Materials*, 190, 918–928. [CrossRef]

[210] Rivera, O. G., Long, W. R., Weiss Jr., CA, Moser, R. D., Williams, B. A., Gore, E. R., & Allison, P. G. (2016). Effect of elevated temperature on alkali-activated geopolymeric binders compared to portland cement-based binders. *Cement and Concrete Research*, 90, 43–51. [CrossRef]

[211] Jiang, X., Xiao, R., Ma, Y., Zhang, M., Bai, Y., & Huang, B. (2020). Influence of waste glass powder on the physico-mechanical properties and microstructures of fly ash-based geopolymer paste after exposure to high temperatures. *Construction and Building Materials*, 262, Article 120579. [CrossRef]

[212] Jaya, N. A., Yun-Ming, L., Cheng-Yong, H., Abdullah, M. M. A. B., & Hussin, K. (2020). Correlation between pore structure, compressive strength and thermal conductivity of porous metakaolin geopolymer. *Construction and Building Materials*, 247, Article 118641. [CrossRef]

[213] Cheng-Yong, H., Yun-Ming, L., Abdullah, M. M. A. B., & Hussin, K. (2017). Thermal resistance variations of fly ash geopolymers: foaming responses. *Scientific Report*, 7(1), Article 45355. [CrossRef]

[214] Wang, J., Basheer, P., Nanukuttan, S., & Bai, Y. (2014). Influence of compressive loading on chloride ingress through concrete," Civil Engineering Research Association of Ireland (CERAI) Proceedings August 2014, Queen's University Belfast, UK.

[215] Zhang, H. Y., Kodur, V., Qi, S. L., Cao, L., & Wu, B. (2014). Development of metakaolin–fly ash based geopolymers for fire resistance applications. *Construction and Building Materials*, 55, 38–45. [CrossRef]

[216] Abdulkareem, O. A., Mustafa Al Bakri, A. M., Kamarudin, H., Khairul Nizar, I., & Saif, A. A. (2014). Effects of elevated temperatures on the thermal behavior and mechanical performance of fly ash geopolymer paste, mortar and lightweight concrete. *Construction and Building Materials*, 50, 377–387. [CrossRef]

[217] Chithambaram, S. J., Kumar, S., & Prasad, M. M. (2019). Thermo-mechanical characteristics of geopolymer mortar. *Construction and Building Materials*, 213, 100–108. [CrossRef]